INVESTIGATION OF AGE DEPENDENT CONTRAST AND T_1 DIFFERENCES IN MR IMAGES AT 3.0 T: A STUDY ON MPRAGE, SPIN ECHO AND FLASH PROTOCOLS

A THESIS SUBMITTED TO
THE GRADUATE SCHOOL OF NATURAL AND APPLIED SECIENCES
OF
MIDDLE EAST TECHNICAL UNIVERSITY

BY

HAYRİYE AKTAŞ

IN PARTIAL FULFILLMENT OF THE REQUIREMENTS
FOR
THE DEGREE OF MASTER OF SCIENCE
IN
BIOMEDICAL ENGINEERING

SEPTEMBER, 2013

Approval of the thesis:

INVESTIGATION OF AGE DEPENDENT CONTRAST AND T_1 DIFFERENCES IN MR IMAGES AT 3.0 T: A STUDY ON MPRAGE, SPIN ECHO AND FLASH PROTOCOLS

Submitted by **HAYRİYE AKTAŞ** in partial fulfillment of the requirements for the degree of **Master of Thesis in Biomedical Engineering Department, Middle East Technical University** by,

Prof. Dr. Canan ÖZGEN _____
Dean, Graduate School of **Natural Applied Sciences**

Prof. Dr. Vasıf HASIRCI _____
Head of Department, **Biomedical Engineering**

Assist. Prof. Dr. Didem GÖKÇAY _____
Supervisor, **Informatics Institue, METU**

Assoc. Prof. Dr. Ewa DOĞRU _____
Co-Supervisor, **Biology Dept., METU**

Examining Committee Members:

Assoc. Prof. Dr. Yeşim SERİNAĞAOĞLU DOĞRUSÖZ _____
Electrics and Electronics Engineering Dept., METU

Assist. Prof. Dr. Didem GÖKÇAY _____
Medical Informatics Dept., METU

Assoc. Prof. Dr. Ewa DOĞRU _____
Biological Sciences Dept., METU

Assoc. Prof. Dr. İlkay ULUSOY _____
Electrics and Electronics Engineering Dept., METU

Prof. Dr. Erkan MUMCUOĞLU _____
Medical Informatics Dept., METU

Date: 03.09.2013

I hereby declare that all information in this document has been obtained and presented in accordance with academic rules and ethical conduct. I also declare that, as required by these rules and conduct, I have fully cited and referenced all material and results that are not original to this work.

Name, Last name : Hayriye AKTAŞ

Signature :

ABSTRACT

INVESTIGATION OF AGE DEPENDENT CONTRAST AND T_1 DIFFERENCES IN MR IMAGES AT 3.0 T: A STUDY ON MPRAGE, SPIN ECHO AND FLASH PROTOCOLS

AKTAŞ, Hayriye

M.Sc., Department of Biomedical Engineering

Supervisor: Assist. Prof. Dr. Didem GÖKÇAY

Co-Supervisor: Assoc. Prof. Dr. Ewa DOĞRU

September 2013, 75 Pages

During healthy aging, the brain undergoes several structural changes such as brain atrophy, decreased volume of GM and WM and increase in CSF volume. These changes introduce prominent low contrast effects to the MRI images of the aging population, causing segmentation problems in the data processing pipeline. Measures of tissue characteristics such as T_1, T_2 provide unique and complementary information to widely used measures of brain atrophy. In this study, image quality metrics such as contrast, SNR, CNR and GWR devised from 3 cortical and 2 sub-cortical regions of interest are used to evaluate the efficiency of MPRAGE and spin echo (SE) scans across ages. Multiple FLASH images are collected with varying flip angles for estimation of T_1 within the GM areas in order to guarantee optimal TR values before the acquisition of SE images. While investigating the results of our parameter selection by calculations on MPRAGE and SE scans, we also utilized whole brain T_1 images computed from multi-contrast FLASH images. As a result, we found that in terms of contrast and gray-white ratios (GWR), T_1 estimated whole brain images are superior to MPRAGE and SE protocols, especially within sub-cortical areas. Furthermore, in T_1 estimated whole brain images, degradation of contrast and GWR due to aging processes is observed to be less pronounced. In our comprehensive evaluation of MPRAGE, SE and FLASH images in young and aged healthy subjects, we observed that T1 estimations derived from FLASH images are useful for improving contrast and GWR.

Keywords: Brain aging, signal-to-noise, contrast, gray-white ratio, MRI parameter adjustment

ÖZ

BEYNİN YAŞLANMASI SÜRECİNE AİT MR GÖRÜNTÜLERİNDE KONTRAST VE T_1 DEĞİŞİKLİKLERİNİN 3.0 T MR CİHAZINDA İNCELENMESİ: MPRAGE, SPIN ECHO VE FLASH PROTOKOLLERİ ÜZERİNE BİR ÇALIŞMA

AKTAŞ, Hayriye

Yüksek Lisans, Biyomedikal Mühendisliği Bölümü

Tez Yöneticisi: Yrd. Doç. Dr. Didem GÖKÇAY

Ortak Tez Yöneticisi: Doç. Dr. Ewa DOĞRU

Eylül 2013, 75 Sayfa

Sağlıklı yaşlanma sürecinde, beyin hacim azalması, GM, WM hacimlerinin azalması ve CSF hacminin artması gibi bazı yapısal değişimlere uğrar. Bu değişimler yaşlanan popülasyonun MRI görüntülerinde belirgin düşük kontrast etkilerini getirir ki bu da veri işleme düzeninde segmentasyon problemlerine neden olur. T_1 ve T_2 gibi doku karakteristiklerinin ölçümü, yaygın olarak kullanılan beyin atrofisi ölçümlerini tamamlayıcı eşsiz bilgiler verir. Bu çalışmada, 3 kortikal ve 2 korteks altı ilgili bölgede kontrast, SNR, CNR ve GWR gibi görüntü kalite ölçütleri T_1 ağırlıklı MPRAGE ve SE görüntülerinin verimliliğini yaş farklarına göre değerlendirmek için kullanılmıştır. SE görüntülerini elde etmeden önce en uygun TR değerlerini garantilemek için ve T_1 kestirimleri için farklı açılarla çekilmiş çoklu FLASH görüntüleri toplanmıştır. MPRAGE ve SE görüntüleri üzerinde hesaplamalar yaparak parametre seçimimizin sonuçlarını değerlendirirken aynı zamanda çoklu kontrasta sahip FLASH görüntülerinden elde edilen tüm beyin T_1 görüntüleri kullanılmıştır. Sonuç olarak, kontrast ve GWR açısından T_1 kestirimi yapılmış tüm beyin görüntüleri MPRAGE ve SE protokollerinden özellikle korteks altı bölgelerde daha iyidir. Ayrıca, T_1 kestirimi yapılmış tüm beyin görüntülerinde yaşlanmaya bağlı olarak kontrast ve GWR daki bozulma MPRAGE ve SE görüntülerine göre daha az belirgindir. Sağlıklı genç ve yaşlı bireylerde MPRAGE, SE ve FLASH görüntülerinin kapsamlı bir analizinde FLASH görüntülerinden elde edilen T_1 kestirimlerinin kontrast ve GWR nun iyileştirilmesinde kullanışlı olduğunu gözlemledik.

Anahtar Kelimeler: Beyin Yaşlanması, sinyal gürültü onayı, kontrast, gri-beyaz oranı, MRI parametrelerinin ayarlanması.

To My Father, Yüksel AKTAŞ

ACKNOWLEDGMENTS

I would like to express my sincere gratitude to my supervisor Asst. Prof. Dr. Didem GÖKÇAY and co-supervisor Assoc. Prof. Dr. Ewa DOĞRU for their guidance, advice, encouragements and support throughout the research.

I would like to thank to all participants for contributions to this study and Bilkent University National Magnetic Resonance Research Center **(**UMRAM) for offering their facilities to conduct MRI scans.

I would like to thank my colleagues and valuable friends Aykut EKEN, Selgün YÜCEİL, Bahar TERCAN, Igor MAPELLI and MRI technician Musa KURNAZ for their friendship and support throughout my study.

I also would like to thank my dear friends Merve KORKMAZ, Merve ERİŞ, Tuğçe TÜRTEN and Ceren BORA for their endless support.

I specially want to thank my fiancé and eternal friend Cemal DİNÇER for his endless patience and love. He always believed in me more than I do throughout this work. I also would like to thank his family for opening their heart and being a family to me.

Finally I would like to thank my dear mother Nermin AKTAŞ for her endless love, and being always there for me. I would especially like to thank my sister Özlem AKTAŞ BALTA, my brothers Hakkı AKTAŞ and Ümit AKTAŞ. Although they live far away from me, I always felt their love and support. I owe my father the greatest gratitude for living an honorable life as an examplar to my own. Without his encouragement, this thesis would not exist.

TABLE OF CONTENTS

ABSTRACT v
ÖZ vi
ACKNOWLEDGMENTS viii
TABLE OF CONTENTS ix
LIST OF TABLES xii
LIST OF FIGURES xiii
INTRODUCTION 1
BACKGROUND 3
2.1 Age Related Morphological Changes 3
2.1.1 Brain Atrophy 4
2.1.2 Gray Matter Alterations Based on Aging 4
2.1.3 Aging Effects on White Matter 5
2.1.4 Age-Induced Alterations in CSF 6
2.1.5 Cortical Thickness in Aging Brain 7
2.2 Age Dependent MRI Signal Alterations 7
2.3 MRI Pulse Sequences 8
The SPIN ECHO Sequence 10
The MPRAGE Sequence 10
The FLASH Sequence 11
Our expectations can be summarized as follows: 12
METHOD 13
3.1 MR Acquisition 13
3.2 T_1 Estimation 14
3.3 Adjustment of Repetition Time (TR) 16
3.4 SNR and Contrast Evaluation on MPRAGE, SE and T_1 Images 17
3.4.1 The Preprocessing of MPRAGE and SE Images 17
3.4.1 T_1 Generation 18
3.4.2 Measurement of Signal within Sub-Cortical and Cortical ROIs 20

Subcortical Landmarks 20
Cortical Landmarks 21
Contrast 22
Signal-to-Noise Ratio (SNR) 23
Contrast-to-Noise Ratio (CNR) 23
Gray-to-White Ratio (GWR) 24
3.5 Comparison Study 24
RESULTS 25
4.1 Subject Profile 25
4.2 Evaluation of Age Dependent Changes via MPRAGE Sequence 25
Cortical Landmarks: 25
Subcortical Landmarks: 26
4.3 Effects of Age Related Changes on SE Images 27
Cortical Landmarks: 27
Subcortical Landmarks: 28
4.4 Age Associated Differences Analyzed on T_1 Estimated Images 29
Cortical Landmarks: 29
Subcortical Landmarks: 30
4.5 Comparison of Spin-Lattice Relaxation Time (T_1) Between Young and Old Participants 31
4.6 Age Effects on Contrast 33
4.6.1 MP-RAGE 33
4.6.2 Spin Echo 33
4.6.3 T_1 Estimated Images 34
4.7 Age Associated Changes in GWR 36
4.7.1 MP-RAGE 36
4.7.2 Spin Echo 36
4.7.3 T_1 Estimated Images 36
4.8 Effects of Age on SNR 41
4.8.1 MP-RAGE 41
4.8.2 Spin Echo 41
4.8.3 T_1 Estimated Images 41
4.9 Age Dependent Changes on CNR 44

4.9.1 MP-RAGE 44
4.9.2 Spin Echo 44
4.9.3 T_1 Estimated Images 44
DISCUSSION 47
5.1 Future Work 50
CONCLUSION 51
REFERENCES 53
GERIATRIC DEPRESSION SCALE 61
TR ADJUSTMENT 65
STUDY INFORMED CONSENT 68
PERSONAL INFORMATION FORM FOR PARTICIPANT 70
APPROVAL OF ETHICS COUNCIL 71
MATLAB CODE OF T_1 ESTIMATION 73

LIST OF TABLES

TABLES

Table 4.1 Participant Demographics 25
Table 4.2 Group Statistics and Independent Samples T Test Results of Cortical Landmarks Measured on MPRAGE images 26
Table 4.3 Group Statistics and Independent Samples T Test Results of Subcortical Landmarks Measured on MPRAGE images 27
Table 4.4 Group Statistics and Independent Samples T Test Results of Cortical Landmarks Measured on SE images 28
Table 4.5 Group Statistics and Independent Samples T Test Results of Subcortical Landmarks Measured on SE images 29
Table 4.6 Group Statistics and Independent Samples T Test Results of Cortical Landmarks Measured on T_1 Estimated Images 30
Table 4.7 Group Statistics and Independent Samples T Test Results of Subcortical Landmarks Measured on T_1 images 31
Table 4.8 Group Statistics and Independent Samples T Test Results of both Subcortical and Cortical Landmarks in Perspective of T_1 Values Variation 32

LIST OF FIGURES

FIGURES

Figure 2.1 Graphs depict age-related volume changes in (a) Gray Matter and (b) White Matter Volume in 116 healthy volunteers (Courchesne, 2000; Huppi et al, 1998). 5
Figure 2.2 (a) Graph shows that total intracranial CSF volume increased with aging. (b) The graph demonstrates %CSF of intracranial space through ageing (Courchesne, 2000). 6
Figure 2.3 Acquiring of the different contrast images by adjusting the TR and TE parameters (Buxton, 2002). 9
Figure 2.4 Example of different cross sections of MPRAGE images at a 3T MRI unit..... 11
Figure 3.1 Data collection and processing pipeline 14
Figure 3.2 The effects of flip angle alterations on contrast 15
(From Left to Right: FA=3˚, FA=5˚, FA=15˚, FA=30˚)..... 15
Figure 3.3 Left: T_1 Estimated Image of a 31 years old subject, Right: T_1 Estimated Image of a 66 years old subject 16
Figure 3.4 The image processing and evaluation pipeline..... 17
Figure 3.5 From left to right: Original image, scaled image, estimated bias field and restored output. 18
Figure 3.6 From Left to Right: Brain Extracted Image, segmented image, GM mask, WM mask. 19
Figure 3.7 Left: T_1 estimated image masked with GM, Right: T_1 estimated image masked with WM. 19
Figure 3.8 From Left to Right: MPRAGE, SE and T_1 Estimated images of the subjects with exactly the same slice locations. 20
Figure 3.9 Subcortical Landmarks: 1: Caudate, 2: Adjacent WM, 3: Putamen..... 20
Figure 3.10 Cortical Landmarks: Left: Blue: Rostral Middle Frontal Gyrus, Red: Adjacent WM, Right: Blue: Crossing Point of Superior Frontal Sulcus and Pre-central Sulcus, Red: Adjacent WM, Green: Posterior Central Gyrus, Purple: Adjacent WM. 21
Figure 3.11 Signal intensity of CSF, GM, WM and fat plotted against TR in a T_1 weighted SE image (Donald, 2003)..... 22
Figure 3.12 Derivation of contrast, signal-to-noise ratio (SNR) and contrast-to-noise ratio (CNR) from ROIs. 23
Figure 4.1 Average Contrast Values of each ROIs. 1: RMFG, 2: SFPC, 3: PCG, 4: Caudate, 5: Putamen. 35
Figure 4.2 Average Scaled GWR Values of each ROIs. 1: RMFG, 2: SFPC, 3: PCG, 4: Caudate, 5: Putamen. 38
Figure 4.3 GWR-Contrast Graphs Distribution of SE, MPRAGE images behavior. and T_1 Estimated Images on cortical level. 39

Figure 4.4 GWR-Contrast Graphs Distribution of SE, MPRAGE images behavior. and T_1 Estimated Images on subcortical level. 40
Figure 4.5 Average SNR Values of each ROIs. 1: RMFG, 2: SFPC, 3: PCG, 4: Caudate, 5: Putamen 43
Figure 4.6 Average CNR Values of each ROIs. 1: RMFG, 2: SFPC, 3: PCG, 4: Caudate, 5: Putamen. 45

CHAPTER 1

INTRODUCTION

The intensity value at a voxel in the MR image is actually the time of the magnetized Hydrogen atoms within that voxel to return to the original position after being tipped by a short pulse.

Since the chemical content of the tissues changes and thereby the amount of the Hydrogen in tissues changes, the relaxation time for each tissue differs. As a result, the three tissue types in the brain Cerebrospinal Fluid (CSF), White Matter (WM) and Gray matter (GM) are represented through different intensity values. The best interest of MR imaging lies in increasing the contrast between GM, WM and CSF. However, due to several factors such as voxel averaging, aging or due to artifacts, the intensity values belonging to these three tissue types may overlap.

Even in the absence of neurological disorder, aging brains show alterations (Driscoll, 2009; Resnick, 2000; Thambisatty, 2010). According to studies conducted recently, these age-dependent alterations affect the imaging properties of the brains (Salat, 2009). Revealing the alterations derived from healthy aging provides crucial foundation for understanding age related brain diseases (Long, 2012; Tau, 2010).

Initial studies on aging brains focused on neuronal loss (Gómez-Isla, 1996; Gómez-Isla, 1997; Giannakopoulos, 1996), but nowadays it is proved that there is no decrease in the number of neurons with aging. Instead, the organizational structure and the functionality of the neurons alter with increasing age (Morrison, 1997; Sachdev, 2003).

Most of the studies in literature have concentrated on morphological changes in healthy aging and reported brain atrophy (Yue, 1997; Coffey, 1992; Murphy, 1992; Raz, 1998; Resnick, 2000). There is a reduction in GM with aging and the decrease in GM volume was reported to be 5% per decade (Courchesne, 2000). Longitudinal analyses also demonstrated a decrease in cortical thickness with aging (Rettman, 2006; Salat, 2004).

On the other hand, the proportion of WM volume to whole brain shows a quadratic pattern of change, slightly increasing until an age of approximately 40 years then decreasing quickly thereafter (Ge, 2002). Once the WM decreases in late life, the rate of decrease seemed to be consistent and fast in comparison with that of GM. In addition, with increasing age, significant increase of lateral and third ventricle volumes were reported (Ylikoski, 1995). Such age related

changes in the brain alter the imaging properties and hence there is a contrast reduction in aged population. This is an important problem which distorts the diagnosis and segmentation procedures. In this thesis work, the improvement of image quality by utilizing the spin-lattice relaxation time T_1 is the main motivating factor.

The intensity difference in MR images serves as an important biomarker of age related diseases as well as healthy aging. Although there is large number of studies evaluating aging brains morphologically, the signal alterations derived from aging is less studied in literature.

In our study, 20 healthy volunteers were scanned with MPRAGE and FLASH sequences, and then T_1 estimation was performed by utilizing these sequences. Accordingly, the most suitable repetition time (TR) was calculated and SE images were obtained with new estimated MRI parameters. Openly available neuroimaging software tools are utilized in the brain extraction, intensity measurement, and registration. For this purpose we used AFNI, FSL, MRIcro.

Finally, in order to evaluate the image quality contrast, gray-white-ratio (GWR), signal-to-noise ratio (SNR) and contrast-to-noise ratio (CNR) were calculated on 9 predefined specific regions of interest (ROI). The outcomes of quality measurements were compared with t-test to exhibit the signal differences between young and old participants.

Layout of topics in this thesis is as follows. Background information about aging and MRI pulse sequences used in this study is given in Chapter 2. At first, age related morphological changes are mentioned followed by signal alterations in aging brains. Then, the theoretical information about MRI pulse sequences is introduced. In Chapter 3, the theory behind the experiments, data collection and analysis phases is explained. The statistical evaluation of image quality metrics which is conducted on participants is provided separately based on MRI sequence, parameter and specific regions in Chapter 4. The results were interpreted, and compared with the literature in discussion part (Chapter 5). In chapter 6, conclusion, a short summary of outcomes of this thesis work and future plans are listed.

CHAPTER 2

BACKGROUND

Aging brains go under some structural changes even without any disorder deteriorating the nervous tissue (Driscoll, 2009; Resnick, 2000; Thambisatty, 2010). Recent studies demonstrated that there is a fundamental change in brain tissue with age that alters the imaging properties of brain structures (Salat, 2009). Revealing alterations derived from healthy aging provides crucial foundation for age related brain diseases (Long, 2012; Tau, 2010).

Until recently, it was supposed that death of neurons was unavoidable consequence of healthy aging. In the early studies, it was thought that volumetric changes in brain during aging were the results of age dependent neuronal loss (Brody, 1970; Coleman. 1987). Most of these studies measured a common characteristic: the researchers evaluated only the density of the neurons at a particular region, not the number of neurons (Morrison, 1997). After the developments of the tools and procedures mediating for counting neurons, especially stereological methods were applied to aging research (Gómez-Isla, 1996; Gómez-Isla, 1997; Giannakopoulos, 1996). The outcome of these studies was unexpected, in such a way that there was not a significant relation between the decrease in neuron number and normal aging at least with respect to most brain regions. To be able to establish this concept, the hippocampus has been studied and it was demonstrated that functional organization of hippocampus was changed with aging (Morrison, 1997; Sachdev, 2003).

Magnetic Resonance Imaging (MRI) has been used extensively in studies of brain aging, because it provides high resolution in vivo images that may aid in the prediction of individuals at risk for memory impairment, Alzheimer's disease (Convit, 1997) and other neurological disorders.

2.1 Age Related Morphological Changes

Within the intracranial area, human brain contains White Matter (WM), Gray Matter (GM) and Cerebrospinal Fluid (CSF). During aging process, brain undergoes several changes and the some indicators of these changes are reported in the volume of White Matter (WM), Gray Matter (GM) and Cerebrospinal Fluid (CSF), intracranial space, whole brain and cortical thickness.

2.1.1 Brain Atrophy

The reduction in brain volume with aging is a well-known fact (Samorajski, 1976; Ho, 1980). With the advances in neuroimaging area, many studies investigated brain atrophy. Whole brain atrophy has been showed in cross-sectional studies likewise atrophy at some anatomical structures (Yue, 1997; Coffey, 1992; Murphy, 1992; Raz, 1998; Resnick, 2000).

There is a significant decrease in total brain volume with aging (Rettman, 2006). Between early childhood and early adolescence, it is found that the healthy brain and intracranial space grew exponentially by about 25%-27%; however, by 71-80 years of age, brain volume was less than that of 2-3-year-old children. These brain growth and aging effects were similar in the male and female volunteers. Intracranial volume increases with brain volume but thereafter, declines with aging (Courchesne, 2000). Age related volume differences are found in; frontal, temporal, parietal-occipital regions with smaller volumes in older versus younger individuals (Rettman, 2006, Thambisatty, 2010). Additionally, with respect to gender, the brain atrophy in males was bigger than females and started earlier (Xu, 2000). Despite from aging, other factors such as chronic alcohol consumption are also shown to play a role in brain atrophy (Harper, 1985; Kril, 1999).

Because brain parenchyma is generally composed of GM and WM, the quantitative analysis of brain atrophy underlying separate GM and WM have important implications for our understanding and monitoring of the aging process in the brain (Ge, 2002).

2.1.2 Gray Matter Alterations Based on Aging

GM increased approximately 13 % from early to later (6-9 years) childhood. Thereafter, GM increased more slowly and reached a plateau in the 4^{th} decade, decreasing again by 13 % in the oldest volunteers (Courchesne, 2000). The decline in the proportion of GM volume to whole brain volume appears to occur by a relatively young age and the decrease is constant and linear. Findings from the post mortem studies in middle and late adult life have suggested that the GM loss (shrinkage) might be correlated with a decrease in the size of large neurons rather than a notable decrease in the number of neurons (Ge, 2002). Age-related cognitive decline is frequently attributed to deterioration of cortical gray matter (GM) structures (Ziegler, 2008). The largest age-related differences are observed in prefrontal GM (Rettman, 2006).

In a quantitative study including 116 participants (age ranged from 19 moths to 80years) the decrease in GM volume was reported 5% per decade (Courchesne, 2000). In a recent study investigating morphological alterations of aging human brain, gray matter atrophy was found on both cortical and subcortical regions with region dependence (Long, 2012).

Raz and colleagues conducted a cross-sectional study and reported the most significant differences in prefrontal GM (Raz, 1997). On the other hand, other studies demonstrated age effects on GM changes in frontal (Coffey, 1992; Mueller, 1998), temporal (Coffey, 1992; Sullivan, 1995; Mueller, 1998) and parietal-occipital (Murphy, 1996) cortices.

2.1.3 Aging Effects on White Matter

The proportion of WM volume to whole brain volume shows a quadratic pattern of change, slightly increasing until an age of approximately 40 years then decreasing quickly thereafter (Ge, 2002). Once the WM decreases in late life, the rate of decrease seemed to be consistent and fast in comparison with that of GM. This finding was also suggested with other studies in which age-related atrophy was greater in WM than in GM, although the time when this volume loss started not investigated (Ge, 2002). In the very old, the decline of the WM volume is disproportionally greater than the decline of the GM volume (Salat, 1999). Findings in GM and WM are not necessarily coincident with each other in terms of timing and extent of tissue loss in brain aging (Ge, 2002). Similar volumetric differences in WM are also reported in Courchesne (2000) as seen in figure 2.1.

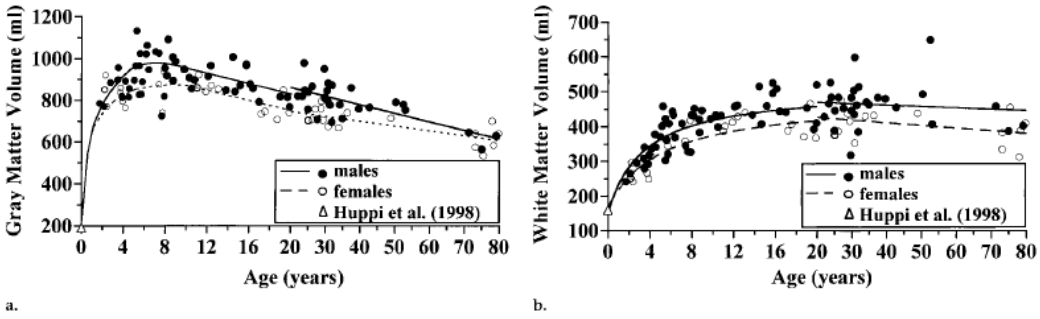

Figure 2.1 Graphs depict age-related volume changes in (a) Gray Matter and (b) White Matter Volume in 116 healthy volunteers (Courchesne, 2000; Huppi et al, 1998).

Age-related WM degeneration is closely related with cognitive and behavioral changes in healthy aging (Salat, 1999). Several studies that examined regional effects of age found that frontal areas showed the greatest volumetric reduction (Ziegler, 2008, Raz, 1997, Salat, 1999).

In a stereological investigation study conducted by Tang et. al. (1997) the total volume of the white matter difference between young and old subjects was found 15% and the total volume of myelinated fibers 17%. The outcome of this study demonstrated that the loss of myelinated fibers having small diameter is the likely cause of reduced WM volume in elderly people (Tang, 1997).

Unlike healthy aging, WM and GM alterations may be correlated with neurological diseases such as extraordinary WM volume in Alzheimer disease (Stout, 1996). In a study conducted by Braffman and colleagues, 23 formalin-fixed brain specimens were analyzed in the aspect of aging and they reported that most of the hyperintense WM lesions were resulted from exquisite demyelination (Braffman, 1988).

In a study composed of 142 healthy subjects (aged between 21-80 years old), WM hyperintensities increased 20% with age in young subgroup 21-30 years old and 100% in old subgroup in 71-80 years old (Christiansen, 1994). Also another study reported an important increase of WM hyperintensity in periventricular region with age in a non-linear pattern but not with gender (Ylikoski, 1995).

Yue et. al. (1997) investigated WM alterations in 3301 old volunteers (65 or older) and demonstrated that simply 4.4% of the participants did not show any abnormality but the majority of the subjects (80%) exhibited significant age related changes (Yue, 1997).

2.1.4 Age-Induced Alterations in CSF

CSF accounts for a small percentage (7%-12%) of the total intracranial volume in a healthy young person. However, in 71-80-year old adults, CSF in the ventricles and leptomeninges can account for 16%-25. The increases in the absolute volume of intracranial CSF are a phenomenon not only in aging but also through the entire life span (Courchesne, 2000). In a study of Coffey and colleagues (1992), it was reported that the third ventricle volume increased 2.8% per year and the enlargement of lateral ventricles was 3.2% per year with aging (Coffey, 1992). In another study composing of 128 neurologically healthy volunteers, significant increase of lateral and third ventricle volumes was also reported (Ylikoski, 1995). The age related changes of intracranial space and CSF can be seen in Figure 2.2.

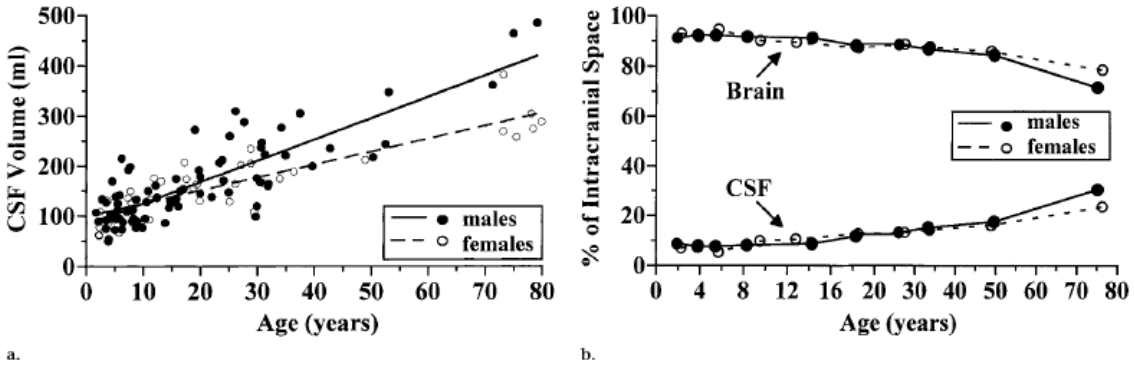

Figure 2.2 (a) Graph shows that total intracranial CSF volume increased with aging. (b) The graph demonstrates %CSF of intracranial space through ageing (Courchesne, 2000).

In a study including evaluation of aging effects on 69 neurologically non-diseased volunteers via PET and MRI techniques, besides the significance of the increase in ventricular and peripheral CSF volumes, the sex differences prominent on male subjects were reported (Murphy, 1996).

In another study, Yue and colleagues conducted a comprehensive research on 3660 elderly volunteers and reported a significant relationship between ventricular enlargement and aging. The increase in ventricular volume with increasing age was observed (Yue, 1997).

There is a contradiction in the literature about gender effects on CSF and intracranial volume behavior with aging. While Resnick (2003) and Courchesne (2000) reported that there was no difference between male and female volunteers, according to Blatter et. al. the age related differences in males were more pronounced (Blatter, 1995).

Positive correlations between age and ventricular size were substantial. Negative correlations between age and total brain, gray and brain volumes were modest, although significant (Resnick, 2000).

To sum up, despite the diversity in the literature in the aspect of both calculated metrics and results there is a strong agreement that there is a significant ventricular enlargement with increasing age and this enlargement starts in males earlier than females.

2.1.5 Cortical Thickness in Aging Brain

Longitudinal analyses have also demonstrated cortical atrophy with age. Findings suggest that there are age related changes in geometric shape of specific cortical and sulcal regions. Age differences in cortical thickness were prominent in the central sulcus (Salat, 2004). More shallow sulci could signify that older individuals have more 'open' sulci than younger individuals - an indication of age associated cortical shape differences (Rettman, 2006).

The cortical thickness of the cortical mantle decreases with increasing age and also there are differences in the shape of cortical surfaces (Magnotta, 1999). Moreover, cortical thinning related to the level of clinical impairment even in the first phases of Alzheimer's Disease (Dickerson, 2008).

2.2 Age Dependent MRI Signal Alterations

It is critical to determine the clinical significance of such changes, and whether signal alterations are general or exhibit selective regional patterns. It is also important to understand how changes in tissue properties relate to alterations in neural morphometry to determine whether signal properties may provide a useful biomarker of age and disease-associated histological and pathological properties (Salat, 2006).

In literature there are different opinions about how gray matter and white matter change with respect to each other in aging. According to both of post mortem and in vivo studies, GM volume divided by WM volume decreases with aging (Courchesne, 2000, Coffey, 1998, Raz, 1997). On the other hand, some studies demonstrated that there is no significant difference in GM WM volume ratio between young and old objects (Ge, 2002). However, it is a fact that the degree of white matter volume reduction is larger than that of gray matter which indicates that GM volume divided by WM volume increases with aging (Salat, 1999, Salat, 2009).

Despite the large number of studies that measure brain space and volume, there is a lack of analogous studies examining how the signal characteristics of different brain tissues are affected by normal or pathological aging. The characterization of signal changes with aging or disease provides important information that is complementary to morphometric studies of regional brain volumes (Davatzikos, 2002).

These results demonstrate that there are strong regional changes in neuronal tissue properties with aging and tissue intensity measures may serve as an important biomarker of degeneration. These alterations in neural morphometry determine that whether signal properties may provide a useful biomarker of age and disease-associated histological and pathological properties (Salat, 2009).

The GWR measures intensity differences between GM and WM: In predefined ROIs, Average GM intensity is divided to average WM intensity to obtain GWR. GWR showed a considerable increase (towards a value of 1) with increasing age, demonstrating an overall decrease in the contrast between these tissue classes, mostly due to a decrease in white matter signal intensity. Factors that may led to signal changes include WM demyelination and changes in water, protein and mineral content of the tissue but these kind of alterations cannot evaluated by standard MRI protocols at cellular basis (Davatzikos, 2002, Salat, 2009).

Fewer studies reported the changes in tissue signal properties, such as T_1 relaxation times and signal intensity (Cho, 1997, Davatzikos, 2002, Salat, 2009). The spin-lattice relaxation time (T_1) of human brain tissue has previously been used as an indicator of brain development or of brain maturation. T_1 declines throughout adolescence and early adulthood, to achieve a minimum value in the fourth to sixth decade of life, then T_1 begins to increase (Cho, 1997). An early study by Raz and colleagues (1997) examined spin-lattice (T_1) relaxation time and found a prolongation in temporal lobe white matter with increasing age. They additionally found that there was a reduction in the differentiation of gray and white matter T_1, and this change in contrast was associated with cognitive performance (Raz, 1997).

The decrease in Contrast Ratio (CR) with age was independent of age-related changes in brain volume. This absence of significant association between longitudinal changes in CR and volumes indicates that tissue contrast measurements provide unique information beyond that of the typically employed volumetric atrophy measurements (Davatzikos, 2002).

Furthermore, the decrease in cortical thinning also affects the signal properties. Specific regions having thinner cortex will be more prone to partial volume effect (PVE), hence the measured signal would be distorted, contributing to the contrast decline in aging brain images.

2.3 MRI Pulse Sequences

All MR images are acquired through unique pulse sequences. A pulse sequence is composed of radiofrequency (RF) pulses and gradient pulses which have precise durations and timings. The main aim of a pulse sequence is to produce contrast between tissue types while avoiding

artifacts. There are various designs of sequences, but they all have timing values called repetition time (TR) and echo time (TE) which can be adjusted.

MRI uses the properties of the Hydrogen which constitutes 75-80 % of the human body. One of the most important properties of the Hydrogen is spin-lattice relaxation time (T_1). T_1 is the relaxation time for the z component of the magnetization vector which comes into thermodynamic equilibrium with its surroundings (the "lattice").

The intensity values observed in MR image is acquired via various forms depending on tissue characteristics and the sequence used during MR scanning. For instance, the intensity in (x,y,z) voxel, I(x,y,z) in a Spin Echo (SE) sequence can be calculated basically as follows:

$$I(x,y,z) = M_0 \, e^{-TE/T2} \, (1 - e^{-TR/T1}) \qquad (2.1)$$

Here, TR, 'repetition time' is the amount of time that exists between successive pulse sequences applied to the same slice. Echo Time (TE) is the time between the first RF pulse and MR signal sampling, corresponding to maximum of echo.

As one can see above formulation, by changing the TE and TR MRI parameters the image contrast characteristics can be controlled. For example, if we want a proton density (PD) weighted intensity value, the role of the M_0 part in formula should be dominated than the other components. Hence, TE and TR should be chosen in such a way that e^{-TE/T_2} term and e^{-TR/T_1} term will converge to 1 (See Figure 2.3, 'Density Weighted'). In order to obtain a T_2 weighted image, since e^{-TE/T_2} term is the main value that affects the intensity therefore TE should be chosen as proportional to real T_2 numbers that can show a contrast. However, TR should be chosen a big number so that the effect of e^{-TR/T_1} term will be weak. As a result e^{-TR/T_1} will be close to zero. (Figure 2.3, 'T_2 weighted'). Similar adjustments can be made to obtain T_1 weighted images, as seen in Figure 2.3.

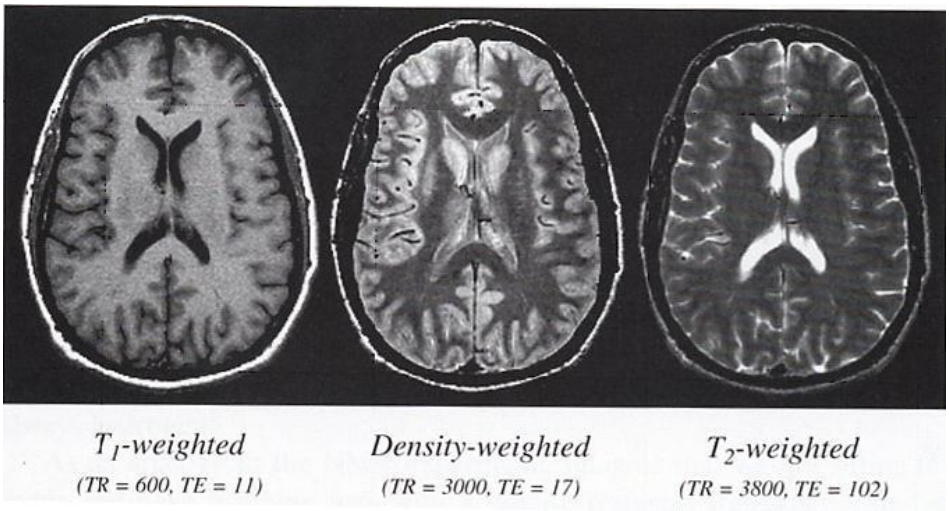

Figure 2.3 Acquiring of the different contrast images by adjusting the TR and TE parameters (Buxton, 2002).

The fundamental factors that determine the contrast in MRI images are M_0, T_1 and T_2 (or T_2*) which are characteristic tissue values.

Usually the operator sets TR and TE to obtain the essential image contrast (Donald, 2003). In neuroimaging, there are three fundamental requirements for structural imaging. First of all, the spatial resolution ought to be high (1mm or better). Second, contrast between white matter (WM) and gray matter (GM) must be attained. Third, acquisition time should not be too long since most of patients cannot bear long durations inside the scanner (Deichmann, 2000). The importance of the short imaging time is discussed in the Manual of the Clinical Magnetic Resonance Imaging, (CMRI) by Heiken et al. (1991). In this manual, it is explained that there are motivations of the development of the rapid imaging techniques based on two factors: improvement of the capability of the clinical MRI and reducing the artifacts which are derived from cardiac, respiratory and other patient motion (Heinken, 1991).

Spin echo (SE) and gradient echo (GE) are accepted as mainstream MRI pulse sequence families. Although the MRI technology was developed more than 30 years, creation of new MRI pulse sequences and improvement is still a focus of interest in order to get images with a better contrast.

The SPIN ECHO Sequence

Radiofrequency spin echo (SE) is one of the two fundamental pulse sequences in MRI. Unlike the MP-RAGE, SE images are typically acquired in the 2D mode. The ability of SE pulse sequence to acquire a specific contrast weighting, T_1-, T_2-, or proton density-weighted, with the combinations of TR and TE values is the most important advantage of this sequence (Hendrick, 1999).

SE also is less prone to the artifacts derived from off-resonance effects such as main magnetic field inhomogeneity and magnetic susceptibility variations than GE.

The MPRAGE Sequence

MPRAGE, abbreviation for Magnetization Prepared Rapid Acquisition by Gradient Echo, is a 3D gradient echo based sequence which is really appropriate for the structural imaging. It has been demonstrated that 3-D MP-RAGE images may yield a good contrast (Runge et al., 1991; Mugler III et al., 1992; Epstein et al., 1994, Frahm et al., 1986). The signal equation of MPRAGE sequence is as follows (Liu, 2011).

$$S = \sum_i Fw(i) M_i \sin\theta \exp(-TE/T_2^*) \qquad (2.2)$$

Fw(i) is the Fourier weight of each k-space line in the voxel, which is determined solely by the phase encoding scheme used by MPRAGE.

MPRAGE images have very high resolution and small anatomical details are good. Figure 2.4 demonstrates a T_1 weighted MPRAGE image in axial, coronal and sagittal slice views respectively. The usage of small flip angles is another advantage which causes to a low specific

absorption rate (SAR), even in studies conducted in high field MRI (greater than 3.0 T) like in our case.

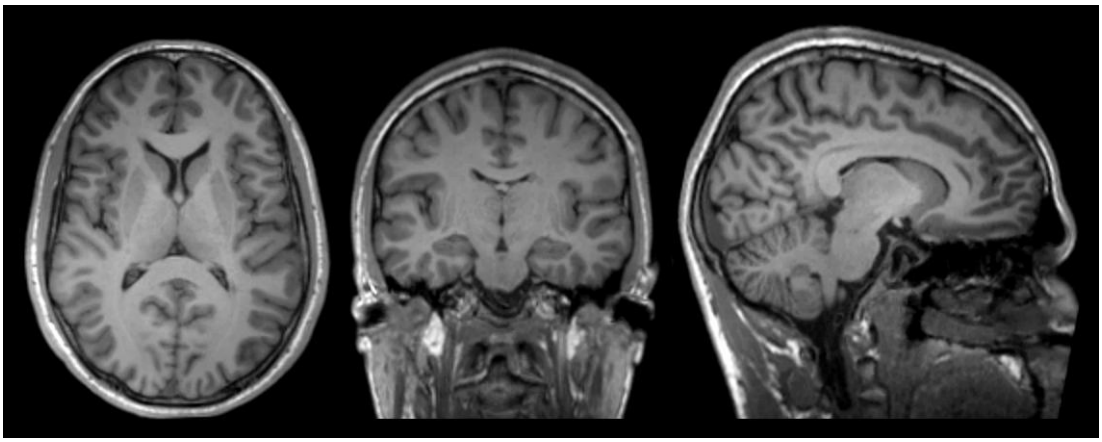

Figure 2.4 Example of different cross sections of MPRAGE images at a 3T MRI unit.

The FLASH Sequence

FLASH MRI (Fast Low Angle SHot Magnetic Resonance Imaging) is a basic measuring principle for rapid MRI invented in 1985 by Jens Frahm, Axel Haase, W Hänicke, KD Merboldt, and D Matthaei at the Max-Planck-Institut für biophysikalische Chemie in Göttingen, Germany. The technique is simple and revolutionary in shortening MRI measuring times. Different manufacturers of MRI equipment use different names for this experiment. Siemens uses the name FLASH, General Electric used the name SPGR (Spoiled Gradient Echo), and Philips uses the name CE-FFE-T1 (Contrast-Enhanced Fast Field Echo) or T1-FFE (T_1-weighted Fast Field Echo). From now on FLASH term will be used in this work.

FLASH is acquired by spoiling Gradient Echo sequences which form the basis for an essential group of imaging methods that find widespread use in clinical practice, particularly when fast imaging is important. RF spoiling can be achieved by different methods. The most straightforward procedure is to choose TR that is at least four to five times T_2; as a consequence the transverse magnetization decays nearly to zero as the outcome of the pulse sequence (Bernstein, 2004).

The steady-state saturation recovery gradient echo sequences like FLASH have several advantages:

1. These images can be expressed easily via well-known equations used for image construction.

2. They can be adjusted in order to yield contrast differences derived from varied intrinsic tissue parameters.

3. Most of MR scanners contain these sequences; they are easily accessible (Fischl, 2004).

Especially for these kind of sequences; S, the signal measured on images acquired via these sequences, can be expressed as a function of the intrinsic tissue parameters $\beta = [T_1, P, T_2^*]^T$ by solving the steady state Bloch equation via:

$$S(m, \beta) = P \sin \alpha \left(\frac{1 - e^{-TR/T1}}{1 - \cos \alpha \, e^{-TR/T1}} \right) \quad (2.3)$$

where $m = [TR, TE, \alpha]^T$ are the acquisition parameters that the user can adjust. In the case of at least as many FLASH images have been collected as there are parameters to be solved for, the estimation of the tissue parameters β is a well-posed problem. In this work, 4 different FLASH images are collected per subject. Thus, the problem is made over-determined by collecting additional measurements which results in less noise in the parameter estimates.

Our aim in this thesis is to investigate thoroughly the contrast changes due to aging, using different pulse sequences. The motivating factor is the reports in the literature regarding contrast loss in the aging population. We wanted to determine how signal differences due to aging processes are manifested in different pulse sequences. Among MR sequences, we decided to use MPRAGE, SE and FLASH which is suitable for T_1 estimation.

Our expectations can be summarized as follows:

- It is expected that there will be contrast differences between young and old subjects in MPRAGE sequence: the contrast in old volunteers will be lower than the young volunteers
- We expect that the contrast of SE with properly adjusted TR will be better than MPRAGE.
- There will be significant differences in T_1 tissue values between young and old individuals (with a prolongation with aging).
- Better contrast is expected in T_1 estimated images than MPRAGE and SE especially in subcortical areas.

Contrast and GWR between tissue types are the two main dependent parameters of our study. High contrast and low GWR are indicators of high quality imaging setups.

CHAPTER 3

METHOD

In this study, the brain MR images of participants were acquired via 3.0 Tesla Siemens Magnetom Trio MR Scanner at the UMRAM MR Center in Bilkent University. First of all, the whole was scanned with Magnetization Prepared Rapid Gradient Echo (MPRAGE) sequence with standard MRI parameters. Then brain images with Fast Low Angle Shot (FLASH) sequence were acquired using multiple flip angles. These four sequences adhere to the same imaging coordinates with the MPRAGE sequence. Then while the participant is lying in the scanner, only one slice was extracted from the MPRAGE and FLASH sequences as a reference slice for T_1 estimation procedure from the FLASH. Using an in-house developed MATLAB code (Appendix F), T_1 characteristic of the given brain was estimated within the GM areas. Finally, Spin Echo scans are collected with optimum TR parameter determined according to estimated T_1 value of the brain.

Investigation of signal characteristics was performed offline afterwards. Segmentation procedure was carried out in FSL environment to the first acquired MPRAGE image and the Spin Echo (SE) images and then Contrast, Signal to Noise Ratio (SNR), Contrast to Noise Ratio (CNR), Contrast and Gray White Ratio (GWR) are calculated for specific landmarks to compare differences across MPRAGE, SE, T_1 estimated images as well as differences across young and old adults.

3.1 MR Acquisition

High resolution 3D MPRAGE images were obtained via 3.0 Tesla Siemens Magnetom Trio MR Scanner, with parameters: TR=2500ms, TE=3.16ms, Bandwidth=199Hz/Pixel, matrix 256*256, Slice Thickness 1mm, 256 slices, FOV=256*256 (axial), Number of Averages=1.

4 FLASH images were acquired with four different flip angles (3˚, 5˚, 15˚, 30˚) at the same scanner, TR=20ms, TE=4.15ms, Bandwidth=199Hz/Pixel, matrix 256*256, with Slice Thickness 3mm, 44 slices, FOV=256*256 (axial), Number of Averages=1).

The MRI parameters used in acquiring of SE images are as follows: TR is variable based on T_1 values of each subject, TE=9.4ms, Bandwidth=199Hz/Pixel, matrix 256*256, Slice Thickness 3mm, 44 slices, FOV=256*256 (axial), Number of Averages=1.

The total duration of the scan session is about 40 minutes, and the data collection pipeline is as illustrated in Figure 3.1.

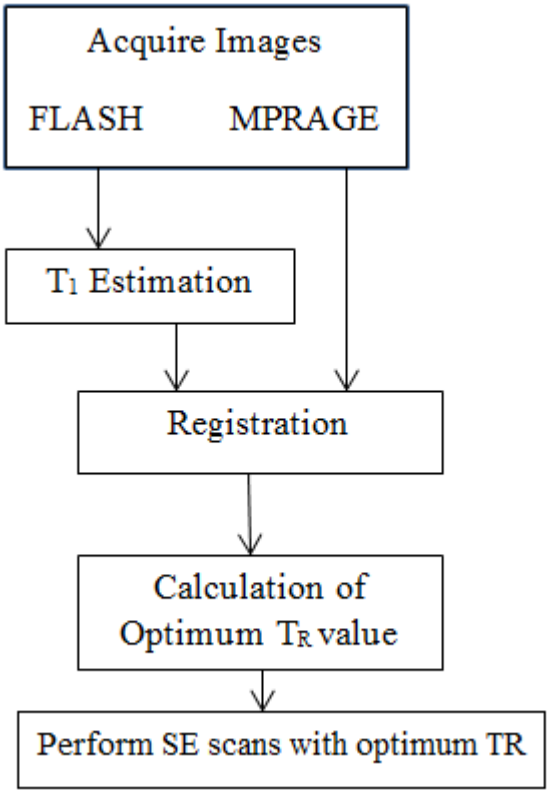

Figure 3.1 Data collection and processing pipeline

3.2 T_1 Estimation

By estimating T_1 characteristics and using them instead of intensity values, contrast between GM, WM and CSF can be increased. To do that at least 3 images should be gathered with three different contrasts. One of the best sequences that provide opportunity to imaging in different contrasts is FLASH (Fischl, 2004).

The intensity value observed in the (x,y,z) voxel of a FLASH image I(x,y,z) can be written in terms of tissue characteristics and scanning parameters TR (repetition time), TE (echo time), α (flip angle) as follows:

$$I(x,y,z) = M_0(x,y,z)\, e^{-TE/T_2^*} \sin(\alpha)(1-e^{-TR/T_1})) \,/\, (1-\cos(\alpha)\, e^{-TR/T_1}) \qquad (3.1)$$

As can be seen in Figure 3.2 the changes in α parameter significantly alter MR contrast.

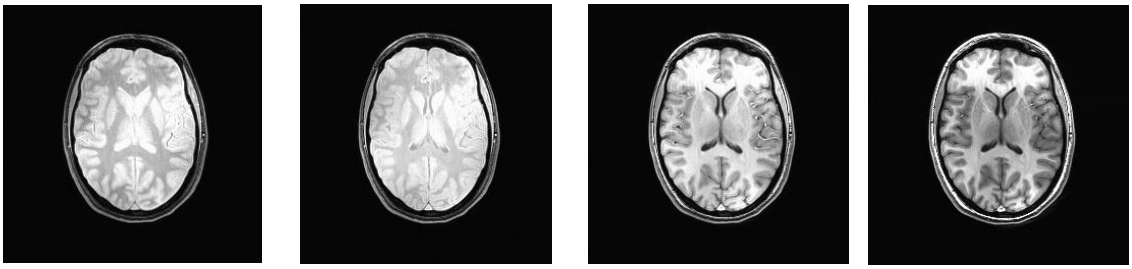

Figure 3.2 The effects of flip angle alterations on contrast

(From Left to Right: FA=3˚, FA=5˚, FA=15˚, FA=30˚)

Our aim is to use the multiple FLASH images for estimating T_1 tissue value for each voxel independently from other voxels. Then, tissue type of voxels can be determined via evaluating T_1 distribution on brain image or using one of the univariate analysis methods (e.g. tresholding method) on the estimated T_1 values instead of intensity value.

In order to estimate the T1 values for each voxel, steps suggested in a preliminary study is carried out (Gökçay, 2004). For really small α values (e.g. α=3˚) the Equation (3.1) can be reduced to equation 3.2 (Buxton, 2002):

$$I(x,y,z) = M_0(x,y,z)\, e^{-TE/T_2^*}\sin(\alpha) \qquad (3.2)$$

In this case, if we describe the intensity value in the image acquired with flip angle=3˚ FLASH equation given in (3.1) through one of the images. Hence, we will not have to estimate T_2* values at all. Now solving the T_1 value for 3 other images by using the remaining parts of the equation is necessary.

The remaining part of the equation is as follows:

$$I_\alpha(x,y,z) = c(\sin(\alpha)/\sin(3))(1-e^{-TR/T_1}) \,/\, (1-\cos(\alpha)e^{-TR/T_1}) \qquad (3.3)$$

In this equation, $I_\alpha(x,y,z)$ is the intensity value in FLASH images with 5, 15 and 30 degrees of α values respectively and c constant is obtained from the intensity value of the image with flip angle 3˚ as provided in equation 3.2. Since TR is a known parameter coming from scanning protocol of the scanner, we need to find T_1 value which is the only unknown parameter by using 3 equations derived from 3 images. This is an over-determined case. We can compute the T_1 value with least squares estimation method as follows:

According to literature the maximum and minimum values that T_1 can have is apparent (e.g. in the widest range 350-4000). In Eq. 3.3, by computing I_5, I_{15}, and I_{30} separately for all of the values that T_1 can take, the expected intensity value of the images can be calculated. Given a specific T_1 value, the difference between the expected intensity versus the actual intensity

observed in I_5, I_{15}, and I_{30} is computed. The T_1 value which provides the least of these squared differences is considered to be the T_1 value belonging to the voxel at hand.

An example T_1 estimated image using this method is given in Figure 3.3. The computer program for the estimation procedure is provided in Appendix F.

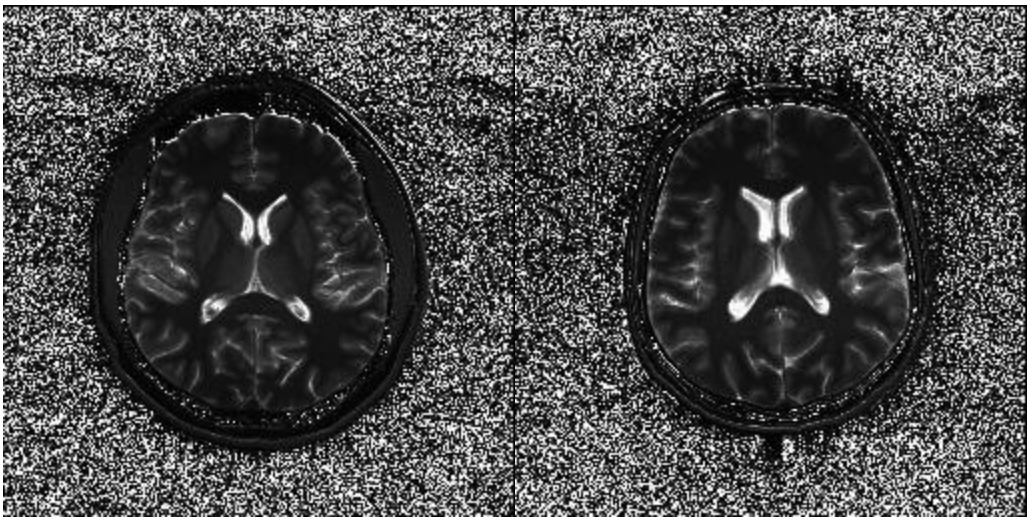

Figure 3.3 Left: T_1 Estimated Image of a 31 years old subject, Right: T_1 Estimated Image of a 66 years old subject

3.3 Adjustment of Repetition Time (TR)

Image contrast characteristics are influenced by the relaxation times which rely on the specific MRI parameters such as TE and TR, as well as the proton density of the tissue. According to (Rosen, 2006) two TR values can be chosen. One of them is equal to half of the average T_1 value of GM (T_{1GM}); the other one is equal to half of the mean of the T_{1GM} and T_{1WM}.

$$TR_1 = T_{1GM} / 2 \quad (3.4)$$

$$T_{1MEAN} = (T_{1GM} + T_{1WM}) / 2 \quad (3.5)$$

$$TR_2 = T_{1MEAN} / 2 \quad (3.6)$$

In order to estimate T_{1GM} and T_{1WM} and calculating the optimum TR to be used in the subsequent SE scans, we transferred one-slice out of the each four FLASH images with different flip angles to the computer and run the MATLAB code given in Appendix F. Only a single slice is used due to time constraints (The subject is lying in scanner during T_1 estimation).

3.4 SNR and Contrast Evaluation on MPRAGE, SE and T_1 Images

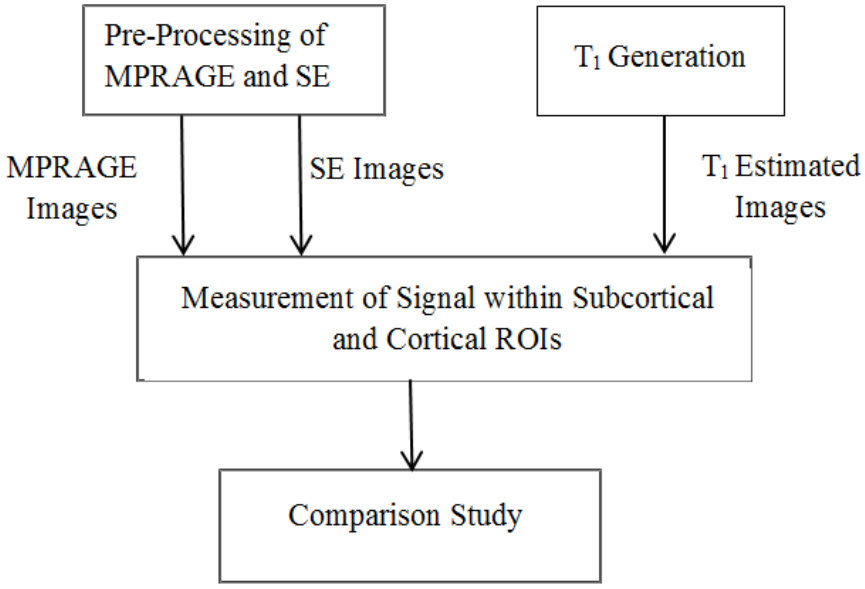

Figure 3.4 The image processing and evaluation pipeline

3.4.1 The Preprocessing of MPRAGE and SE Images

3.4.1.1 Intensity Normalization

Intensity normalization is a really important issue in image analysis studies, especially if the study is built on extracting features based on intensity (Sintorn, 2010).

After converting image types (e.g. from Dicom to NIfTI, NIfTI to AFNI file (+orig.BRIK and +orig.HEAD)) the first step of preprocessing is normalizing the intensities of images acquired from different MRI sequences. Intensity normalization is sometimes named as 'Histogram Stretching' or 'Contrast Stretching'. The Spin Echo and MPRAGE images were scaled to 0-1000 range in order to have a comparable level via '3dcalc' command of AFNI (Cox, 1996).

The normalization was conducted by a multiplicative operation to acquire images at the same gray levels. Each pixel in an image was multiplied by 1000/(maximum value of the current image). 1000 was chosen arbitrarily and the information about the maximum value of the image was obtained by using '3dinfo' command of AFNI.

3.4.1.2 Semi-Automated Removal of Skull and Non-Brain Parts

Then, using FSL the brain extraction (BET) was applied with '-B' option which attempts to reduce image bias, and residual neck voxels (Smith, 2002). This process provides a basis for a

better segmentation. Finally, FAST tool of the FSL was used with 'Restored input' option; this gives the estimated restored input image after correction for bias field (Zhang, 2001).

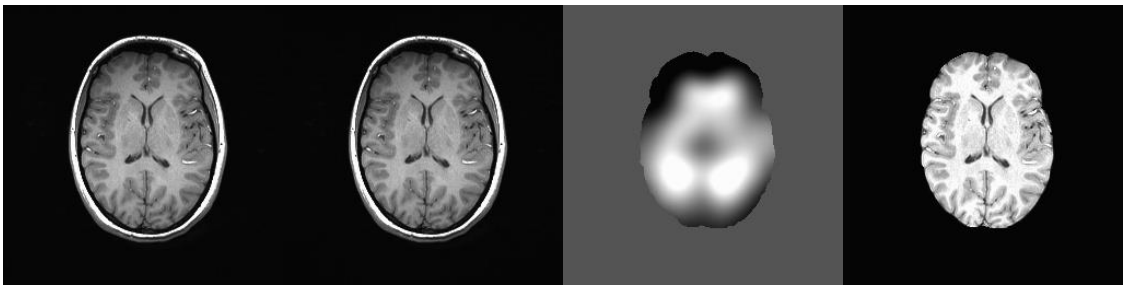

Figure 3.5 From left to right: Original image, scaled image, estimated bias field and restored output.

3.4.1 T_1 Generation

T_1 estimation for whole brain images from FLASH sequences was performed offline using the method described in section 3.2. The resulting image contains the estimated T_1 values of each voxel and this image matrix was converted to DICOM (Digital Imaging and Communications in Medicine) format (.dcm extension) via Dicom toolbox available on Mathworks website.

The MPRAGE image which has the same slice location with FLASH images is also in DICOM format. These two images were converted to NIfTI format (Neuroimaging Informatics Technology Initiative) by using dcm2nii GUI embedded in MRIcro (Rorden, 2005) in order to process the images in AFNI and FSL. Then, the data in NIfTI format were transferred to UNIX environment. These two images were always in different orientation, after saving the images as AFNI file (+orig. file extension) the alignment was accomplished by using AFNI program @Align_Centers. Later, BET (Brain Extraction Tool) which deletes non-brain tissue from an image of the whole head was used for the anatomical image (MPRAGE (Smith, 2002). After brain extraction, FAST (FMRIB's Automated Segmentation Tool) was used to estimate the bias field maps as well as segmenting the MPRAGE into GM, WM, and CSF classes (Zhang, 2001). Figure 3.6 shows the brain extracted and segmented image, respectively. FAST also has the ability to give an output per each tissue class and these are binary images which will be used as a mask later. The GM mask and WM mask can be seen in Figure 3.6, respectively.

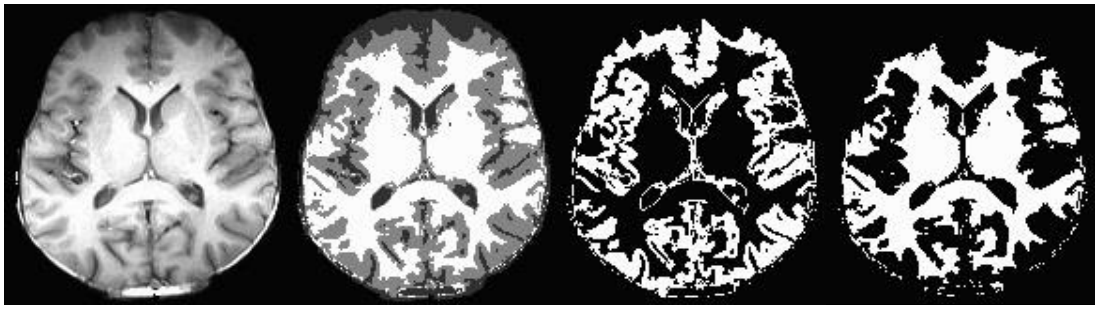

Figure 3.6 From Left to Right: Brain Extracted Image, segmented image, GM mask, WM mask.

In order to obtain T_1 values of GM, AFNI's calculator program '3dcalc' was used. This program does voxel-by-voxel arithmetic on 3D datasets and by using '-expr' option, T_1 estimated image and GM mask were multiplied. The resulting image contains T_1 values of only GM and everything else is zero. The overall average of these T_1 values for the entire brain, T_{1GM} was calculated via 'fslstats' which is one of the FSL command-line utilities. This command was used with '–M' option which calculates the mean of nonzero pixels. The same procedure was applied for calculation of overall T_{1WM} values for the entire brain. Figure 3.7 shows the T_1 image overlaid by GM mask and WM mask respectively.

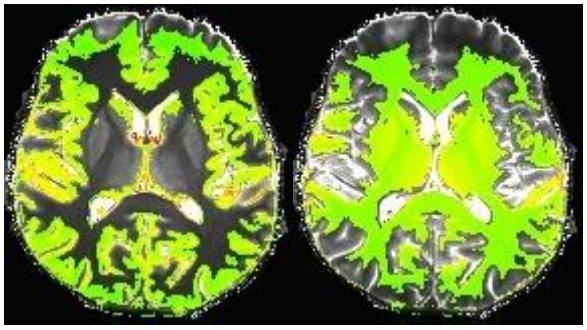

Figure 3.7 Left: T_1 estimated image masked with GM, Right: T_1 estimated image masked with WM.

Subsequent data processing steps proceeded with MPRAGE, SE and T_1 images, for which an example is shown below.

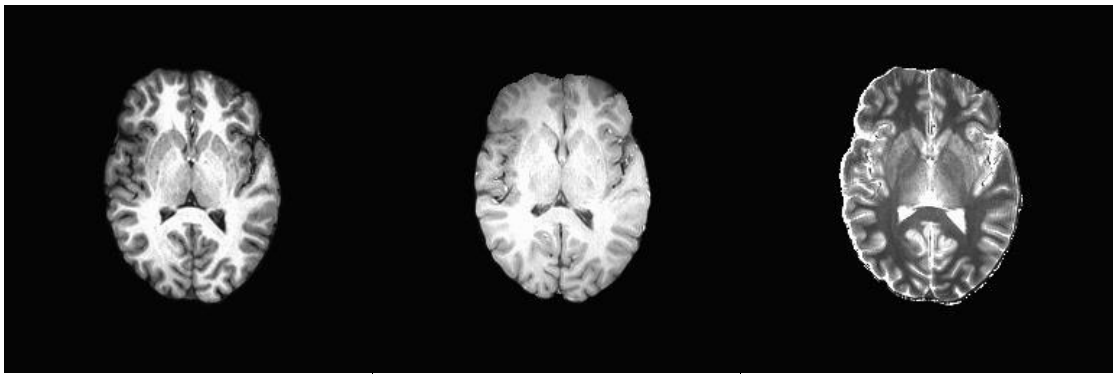

Figure 3.8 From Left to Right: MPRAGE, SE and T_1 Estimated images of the subjects with exactly the same slice locations.

3.4.2 Measurement of Signal within Sub-Cortical and Cortical ROIs

3.4.3.1 Landmark Selection

To be able to evaluate image quality, two subcortical and three cortical landmarks were defined. These landmarks are chosen for the purpose of showing the most important age dependent alterations in tissue characteristics.

Subcortical Landmarks

The Caudate and Putamen were landmarks much studied in literature to accomplish validation. These two structures are good examples of subcortical GM and adjacent WM between Caudate and Putamen (CP_WM) were picked up due to bias field concerns. Figure 3.9 demonstrates the subcortical ROIs. The exact slice of these three landmarks was chosen as the first slice that nucleus accumbens was visible on axial slices while we view the axials from superior to inferior order. CP_WM ROI adheres to internal capsule in between the Caudate and putamen ROIs.

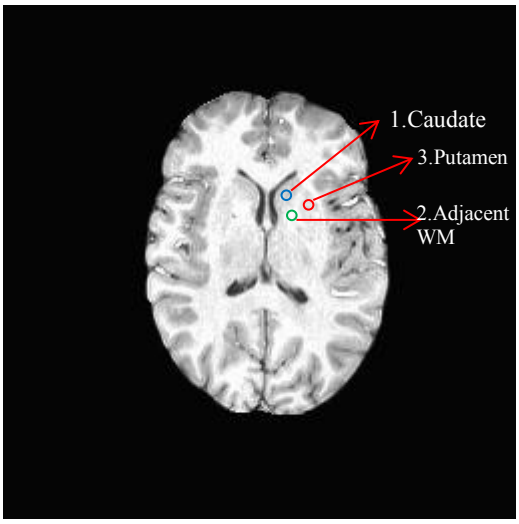

Figure 3.9 Subcortical Landmarks: 1: Caudate, 2: Adjacent WM, 3: Putamen

Cortical Landmarks

There are three different chosen from frontal, superior and posterior aspects of the brain.

First landmark is Rostral Middle Frontal Gyrus (RMFG) which has a strong reduction in white matter but not gray matter (Salat, 2009) in aging. The rostral boundary of the middle frontal gyrus is defined when the first slice of the superior frontal sulcus becomes apparent while we move from the superior extreme of the brain downwards viewing axials. The medial boundary of this landmark is superior frontal sulcus and lateral boundary is the inferior frontal sulcus (Christine Fennema-Notestine, (NeuroLex).

The second landmark is on Post-Central Gyrus (PCG) which is a prominent structure in the parietal lobe; the primary sensory area of the cerebral cortex. The axial slice was chosen as the first slice that handbump area was visible. The rostral boundary of PCG is the appearance of the central sulcus and the disappearance is the caudal boundary of the posterior central gyrus (NeuroLex).

The third one is the crossing point of superior frontal sulcus and pre-central sulcus (SFPC). This is an easy defined important landmark in human brain. The superior frontal sulcus is the sulcus between the superior frontal gyrus and the middle frontal gyrus. The pre-central sulcus stands parallel to the central sulcus, as the name refers, located in front of the central sulcus. The axial slice was chosen as the first slice that handbump area was visible. According to a study by Salat et. al. the superior frontal gyrus showed a remarkable signal change with age (Salat, 2009).

For all of these three cortical landmarks the adjacent WM were also drawn. The Figure 3.10 shows these cortical landmarks.

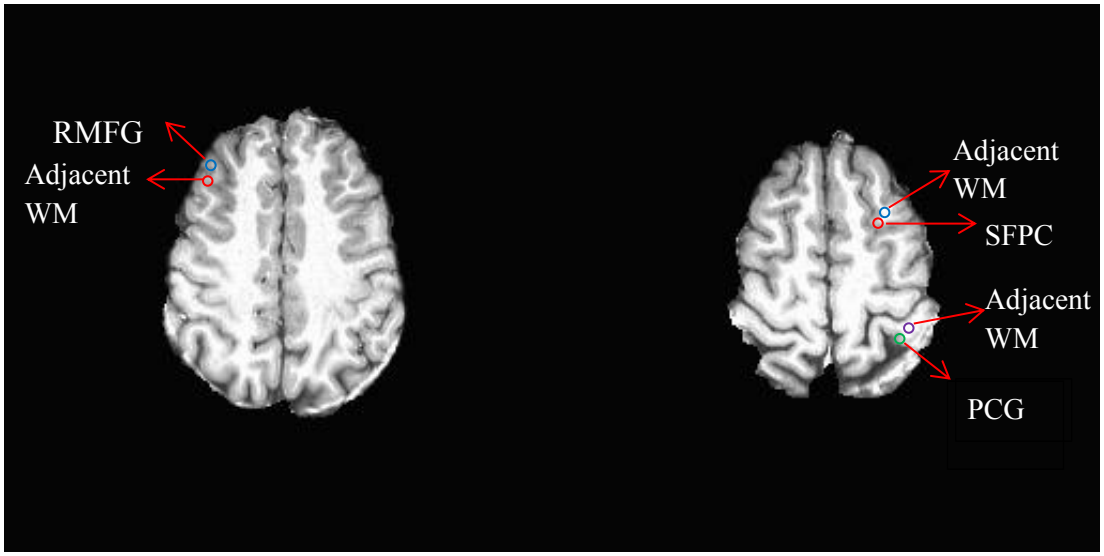

Figure 3.10 Cortical Landmarks: Left: Blue: Rostral Middle Frontal Gyrus, Red: Adjacent WM, Right: Blue: Crossing Point of Superior Frontal Sulcus and Pre-central Sulcus, Red: Adjacent WM, Green: Posterior Central Gyrus, Purple: Adjacent WM.

3.4.3.2 Contrast, Signal-to-Noise Ratio (SNR), Contrast-to-Noise Ratio (CNR), and Gray-to-White Ratio (GWR) Measurements

Contrast

Different tissues have different signal intensities (or brightness) in MR images as visualized by image contrast. By the usage of different pulse sequences or by controlling timing parameters of these sequences, a wide range of contrasts can be produced. The Figure 3.11 shows the signal intensities of different tissue types on T_1-weighted images plotted against TR. With smaller TR values it is easier to differentiate the GM and WM signals, but at longer TR values distinguishing these two tissues is getting harder.

The mathematical formulation of the image contrast is as follows (Donald, 2003):

$$\text{Contrast} = (S_{WM}-S_{GM})/(S_{WM}+S_{GM}) \tag{3.7}$$

Where S_{WM} and S_{GM} are the mean intensities of white matter and gray matter respectively, which measured from small ROIs. As WM and GM signal values get closer to each other, contrast goes to zero.

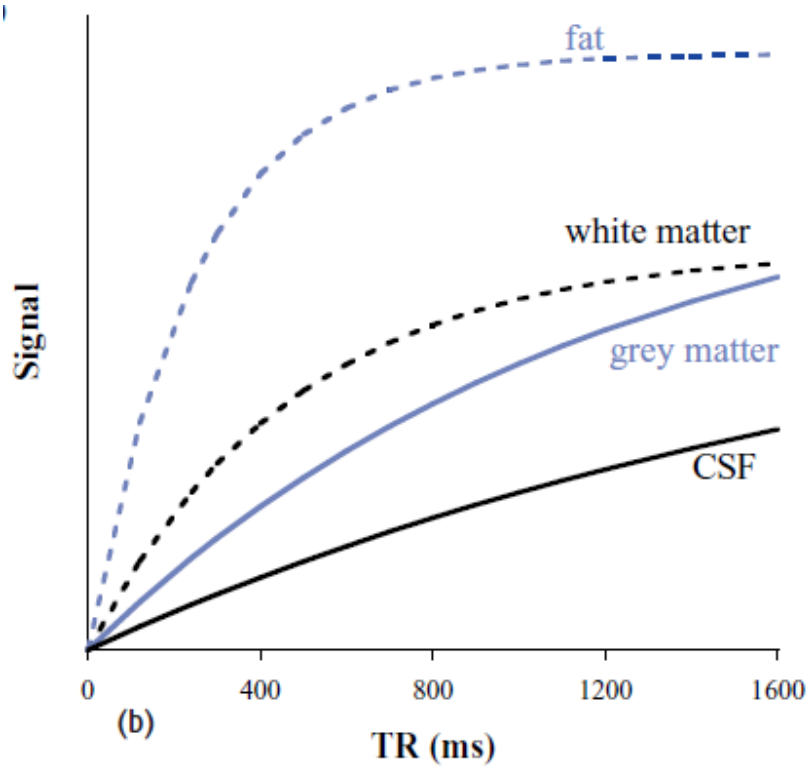

Figure 3.11 Signal intensity of CSF, GM, WM and fat plotted against TR in a T_1 weighted SE image (Donald, 2003).

Signal-to-Noise Ratio (SNR)

The individual voxels that constitute an MR image contain a combination of signal and noise. In principle, noise is not avoidable. It can be derived from electromagnetic noise in the voxel caused by movement of charged particles and non-ideal conditions in the measurement electronics. Signal-to-Noise Ratio is a measure of image quality that is calculated by dividing the mean of tissue intensity to the standard deviation of background noise (measured on the ROI placed outside the object in the image background) (Lu, 2005)[1].

$$SNR = S_{MEAN} / SD_{noise} \quad (3.8)$$

Contrast-to-Noise Ratio (CNR)

The Contrast-to-Noise Ratio is a measure of the combination of both contrast and SNR. The difference between SNR values of two tissue types gives information about CNR (Lu, 2005).

$$CNR = SNR_{WM} - SNR_{GM} \quad (3.9)$$

In our study, the signal values of GM and WM are averaged values of 4 voxels that are arbitrarily chosen within each ROI.

For calculating SD_{noise}, a region of interest was drawn at the upper right corner of one slice from one brain image. This ROI was copied to five slices equally distributed over the volume. The average standard deviation of the background signal was measured in this way in all images in order to get rid of distortion effects such as bias field inhomogeneity.

Figure 3.12 Derivation of contrast, signal-to-noise ratio (SNR) and contrast-to-noise ratio (CNR) from ROIs.

[1] Another way of calculation SNR is to dividing mean signal of tissue to the mean noise. In this study both of these methods were used and the results were compared by Independent t-test analysis in SPSS (George, 2003) and the values derived from Equation 3.8 gave statistically more significant results.

Gray-to-White Ratio (GWR)

The GWR is an important metric to evaluate the gray white matter differentiation in an MR image. The power of this metric comes from the dependence on only mean of the tissue signals, not noise. Although the images were bias field corrected in the preprocessing procedure, having a noise free measurement is still important. The GWR is calculated according to Equation 3.10 (Salat, 2009). In the worst case, the intensities of two different tissues would be equal and the GWR approximates to 1. The absolute distance from 1 gives the information about the differentiability of the tissues.

$$GWR = S_{GM}/S_{WM} \tag{3.10}$$

3.5 Comparison Study

The statistical analysis of measured signals of 5 landmarks from 3 different images (MPRAGE, SE, T_1 estimated) was performed in SPSS. Independent samples t-test was used for mean comparison among young and old subjects. The confidence interval was chosen 95% for all of the analysis in this study.

CHAPTER 4

RESULTS

4.1 Subject Profile

10 young, 10 old healthy volunteers participated in this study (8 male, 12 female; age ranged between 27 and 77). All participants signed informed consent given in Appendix C which is approved by Ankara University School of Medicine Ethical Committee (given in Appendix E). All of the subjects reported no clinical evidence of neurologic disease. One of the young subjects was excluded from study because of abnormal ventricular enlargement. Also Geriatric Depression Scale (Ertan, 2000) was applied to old subjects, and according to test results all of them are healthy aged individuals. The information about the test and demographic information about the subjects are available in Table 4.1.

Table 4.1 Participant Demographics

	N	Age	GDS Score
Young Adults	9 (6 Male/ 3 Female)	31.33±4.59 (Ranged 27-43)	-
Old Adults	10 (2 Male/ 8 Female)	68.5±4.24 (Ranged 65-77)	8.2 ± 3.65

Age dependent changes in the signal to noise ratios, cortical and subcortical landmarks are investigated using mean intensity and estimated T_1 values from within the ROIs described in the methods chapter.

4.2 Evaluation of Age Dependent Changes via MPRAGE Sequence

Cortical Landmarks:

To be able to evaluate aging effects on tissue signals and image quality on MPRAGE images 3 predefined ROIs were drawn. According to mean signals and noise information 5 different metric were measured, then Independent Samples T Test analysis was conducted on SPSS

environment for comparison of means of young and old groups. The test results can be seen on Table 4.2.

Table 4.2 Group Statistics and Independent Samples T Test Results of Cortical Landmarks Measured on MPRAGE images

	AGE	N	Mean	Std. Deviation	Std. Error Mean	F	t	p
SNR_{WM}	Young	27	117.47	21.901441	4.214934	1.609	1.980	.053
	Old	30	104.46	27.080061	4.944120			
SNR_{GM}	Young	27	79.20	18.168330	3.496497	.808	-.932	.356
	Old	30	84.22	22.057462	4.027123			
CNR	Young	27	38.26	10.562621	2.032777	2.305	7.276	.000
	Old	30	20.24	8.087224	1.476518			
CONTRAST	Young	27	.198	.053621	.010319	3.563	7.727	.000
	Old	30	.10733	.033598	.006134			
GWR	Young	27	.66937	.075660	.014561	1.647	-7.80	.000
	Old	30	.80493	.054803	.010006			

According to test results there is no statistically meaningful difference between young and old participants in terms of SNR_{GM} on cortical surface ($p>.05$). In SNR_{WM} measurements, the difference in young and old population is almost significant ($p=.053$). However, there is a significant distinction between two age groups in contrast, CNR and GWR measurements ($p\leq.01$).

Subcortical Landmarks:

2 different ROIs were analyzed to evaluate influence of age in subcortical level on MPRAGE images. For image quality assessment SNR, CNR, contrast and GWR parameters were calculated depending on mean signals and noise acquired from ROI calculations. The outcomes of the group statistics and independent t-test analysis are demonstrated in Table 4.3.

Table 4.3 Group Statistics and Independent Samples T Test Results of Subcortical Landmarks Measured on MPRAGE images

	AGE	N	Mean	Std. Deviation	Std. Error Mean	F	t	p
SNR_{WM}	Young	18	143.86389	16.734851	3.944442	1.871	4.035	.000
	Old	20	123.98200	13.606456	3.042496			
SNR_{GM}	Young	18	109.98722	15.668744	3.693158	6.159	3.705	.001
	Old	20	94.19500	9.519713	2.128672			
CNR	Young	18	33.87667	7.491681	1.765806	5.523	1.931	.063
	Old	20	29.78700	5.228236	1.169069			
CONTRAST	Young	18	.14399	.020047	.004725	2.450	1.698	.098
	Old	20	.13450	.014204	.003176			
GWR	Young	18	.74828	.030692	.007234	1.494	-1.35	.183
	Old	20	.76035	.024066	.005381			

The bad contrast in subcortical region is a well-known fact, as expected the differentiation gray and white matter in subcortical regions is worse than in cortical. Also in the aspect of CNR, contrast, GWR there is not a statistically meaningful difference between young and old subjects. However, a meaningful difference between young and old subjects is existed in SNR for GM and WM.

4.3 Effects of Age Related Changes on SE Images

Cortical Landmarks:

Measurements from 3 predefined landmarks (Rostral middle frontal gyrus, Crossing point of superior frontal sulcus and pre-central sulcus, posterior central gyrus) on SE images were used for the investigation of aging effects. The output of the group statistics and independent samples t-test is shown in Table 4.4.

Table 4.4 Group Statistics and Independent Samples T Test Results of Cortical Landmarks Measured on SE images

	AGE	N	Mean	Std. Deviation	Std. Error Mean	F	t	p
SNR_{WM}	Young	27	193.66593	81.433551	15.671894	.010	1.140	.259
	Old	30	170.83600	69.776848	12.739451			
SNR_{GM}	Young	27	157.54815	68.929267	13.265444	.000	.537	.593
	Old	30	148.34633	60.422848	11.031652			
CNR	Young	27	35.89556	16.138955	3.105943	.198	2.719	.009
	Old	30	24.20600	16.269465	2.970384			
CONTRAST	Young	27	.10460	.028556	.005496	1.254	3.137	.003
	Old	30	.07763	.035513	.006484			
GWR	Young	27	.80904	.045835	.008821	2.642	-3.543	.001
	Old	30	.87280	.082752	.015108			

CNR, contrast and GWR showed a meaningful difference between young and old participant groups. But SNR values of GM and WM do not have a meaningful difference among young and old subjects. As can be seen above, signal to noise ratio of WM and GM in SE is better than MPRAGE sequence.

Subcortical Landmarks:

Caudate and Putamen signal intensities were calculated to analyze contrast properties of subcortical areas on SE images. Like it was previously conducted SNR_{WM}, SNR_{GM}, contrast, GWR were calculated, the resulting values were processed in SPSS to compare the means via independent samples t-test. The outcome of the group analysis and t-test are interpreted in Table 4.5.

Table 4.5 Group Statistics and Independent Samples T Test Results of Subcortical Landmarks Measured on SE images

	AGE	N	Mean	Std. Deviation	Std. Error Mean	F	t	p
SNR_{WM}	Young	18	208.98778	85.085411	20.054824	.136	.448	.656
	Old	20	196.29500	88.885129	19.875319			
SNR_{GM}	Young	18	190.16500	78.912901	18.599949	.070	.389	.699
	Old	20	180.06500	80.731983	18.052220			
CNR	Young	18	18.82278	8.095923	1.908227	1.738	-.464	.646
	Old	20	20.25750	10.639134	2.378983			
CONTRAST	Young	18	.04906	.014806	.003490	.222	-.982	.333
	Old	20	.05425	.017492	.003911			
GWR	Young	18	.85394	.191941	.045241	2.662	-.970	.338
	Old	20	.89600	.027606	.006173			

No significant difference was observed between young and old individuals on SE images in any of the parameters. This is not only because of evaluating subcortical regions but also studying on SE sequence. In literature there are lots of papers claiming that SE contrast is worse at 3.0 T.

4.4 Age Associated Differences Analyzed on T_1 Estimated Images

Cortical Landmarks:

After experiments ended, whole brain T_1 estimation was carried out in the laboratory for all of the participants. The T_1 estimated images contain T_1 value of each pixel instead of intensity value. The same landmarks for cortical measures as described earlier were chosen and SNR_{WM}, SNR_{GM}, contrast, GWR were calculated in the same manner. The statistical evaluation results are presented on Table 4.6.

Table 4.6 Group Statistics and Independent Samples T Test Results of Cortical Landmarks Measured on T_1 Estimated Images

	AGE	N	Mean	Std. Deviation	Std. Error Mean	F	t	p
SNR_{WM}	Young	27	.31089	.087246	.016791	.973	-5.382	.000
	Old	30	.45743	.114714	.020944			
SNR_{GM}	Young	27	.73730	.235276	.045279	.258	-3.838	.000
	Old	30	.98077	.242579	.044289			
CNR	Young	27	.42641	.215088	.041394	.301	-1.567	.123
	Old	30	.52117	.238941	.043624			
CONTRAST	Young	27	.491826	.6515192	.1253849	2.378	1.022	.311
	Old	30	.368137	.1185661	.0216471			
GWR	Young	27	2.45356	.818388	.157499	2.552	.711	.480
	Old	30	2.31507	.649553	.118592			

According to statistical analyses, SNR_{GM} and SNR_{WM} demonstrated really significant differences among young and old groups. Although the other parameters seem to not a metric for comparison of the aging impact on healthy individuals, the mean values of the parameters among the groups are much higher than MPRAGE and SE. One important point to highlight is the range of GWR. Since the tissue intensities are used while calculating GWR in MPRAGE and SE the GWR is smaller than 1 ($S_{GM}<S_{WM}$). Whereas in a T_1 estimated image this ratio is bigger than 1 because the spin-lattice relaxation time of GM is bigger than of WM.

Subcortical Landmarks:

New ROIs were drawn on T_1 estimated images for the assessment of image quality at subcortical level. The comparison of means in aspect of image quality was conducted via independent samples t-test on SPSS environment and the results of this analysis can be seen on Table 4.7.

Table 4.7 Group Statistics and Independent Samples T Test Results of Subcortical Landmarks Measured on T_1 images

	AGE	N	Mean	Std. Deviation	Std. Error Mean	F	t	p
SNR_{WM}	Young	18	.55500	.049823	.011743	4.061	-4.273	000
	Old	20	.69020	.125498	.028062			
SNR_{GM}	Young	18	.78883	.066817	.015749	4.451	-3.866	.001
	Old	20	.93900	.158788	.035506			
CNR	Young	18	.23383	.030910	.007286	19.883	-.775	.446
	Old	20	.24880	.080024	.017894			
CONTRAST	Young	18	.199039	.0926922	.0218478	.369	1.936	.061
	Old	20	.153475	.0474874	.0106185			
GWR	Young	18	1.36711	.311136	.073336	.002	.328	.744
	Old	20	1.34020	.184115	.041169			

It is important to note that the SNR of GM and WM do not carry comparable values between MPRAGE/SE and T_1 estimations. This is because the background area on the T_1 estimated images are extremely noisy. Although the contrast and GWR values of the T_1 estimated images are more acceptable than that of MPRAGE and SE, calculation of SNR using a different metric or ROI might be necessary for a thorough validation.

Like in cortical surface measurements, CNR, contrast and GWR did not show a remarkable difference between young and old participants ($p>.05$). There is a noteworthy difference among young and olds in SNR measurements.

Besides having a good contrast, one of the most important advantages of T_1 mapping is the usage in estimating optimum MRI scan parameters. Dealing with the properties of the underlying tissue characteristics gives better contrast as can be seen above.

4.5 Comparison of Spin-Lattice Relaxation Time (T_1) Between Young and Old Participants

In order to accomplish the investigation of spin-lattice relaxation time alterations in aged subjects, all of the five landmarks (2 subcortical, 3 cortical) were evaluated in both and young subjects. Contrary to previous analyses, only mean pixel values were calculated to be able to

compare the T_1 values in two age groups and the statistical analysis was performed. The results of the independent t-test examination were depicted in Table 4.8.

Table 4.8 Group Statistics and Independent Samples T Test Results of both Subcortical and Cortical Landmarks in Perspective of T_1 Values Variation

	AGE	N	Mean	Std. Deviation	Std. Error Mean	F	t	p
Caudate	Young	9	1213.2222	95.37610	31.79203	.461	-2.226	.040
	Old	10	1331.4750	130.99414	41.42398			
CP_WM	Young	9	848.3611	63.61224	21.20408	.484	-3.500	.003
	Old	10	979.3000	94.46037	29.87099			
Putamen	Young	9	1219.8611	72.63297	24.21099	3.103	-2.423	.027
	Old	10	1339.4250	130.76787	41.35243			
RMFG	Young	9	895.4722	332.64117	110.88039	.548	-4.048	.001
	Old	10	1593.2500	409.25980	129.41931			
RMFG_WM	Young	9	579.1667	209.57602	69.85867	4.338	-2.271	.036
	Old	10	757.9500	128.14704	40.52365			
PCG	Young	9	1438.1667	371.39597	123.79866	.092	1.413	.176
	Old	10	1220.6000	299.22317	94.62267			
PCG_WM	Young	9	517.0833	152.89840	50.96613	.221	-.565	.579
	Old	10	564.5500	205.77151	65.07066			
CSFPCG	Young	9	971.2278	259.11581	86.37194	3.934	-3.807	.001
	Old	10	1512.9750	348.57405	110.22879			
CSFPCG_WM	Young	9	479.8333	197.59733	65.86578	.000	-1.932	.070
	Old	10	633.3750	147.58262	46.66972			

Estimated T_1 values were compared between young and old participants in specific structure base. T_1 prolongation with aging was an expected result, hence 8 landmarks out of 9 showed prolonged values with increasing age.

Caudate, Caudate and Putamen adjacent WM, Rostral Middle Frontal Gyrus, Rostral Middle Frontal Gyrus adjacent WM and crossing point of Superior frontal sulcus with Pre-central sulcus showed a statistically meaningful difference between young and old subjects. Only Posterior Central Gyrus and crossing point of Superior frontal sulcus with Pre-central sulcus adjacent WM did not seem to be a distinguishing parameter for examination of behavior of the spin-lattice relaxation time in young and old participants. Except for Posterior Central Sulcus, T_1 values measured on all of the landmarks showed an increase with aging.

In the sections below we will focus on the primary research question in this study: which protocol fares better in terms of contrast and gray white ratio (GWR)? Goodness of the protocol should be implicated by high contrast and GWR lower than 1. In addition, no degradation of these measures should be observed in old adults compared to young. In other words, the contrast and GWR ratios of both populations should be as indistinguishable as possible, for acceptable imaging.

4.6 Age Effects on Contrast

Figure 4.1 depicts the average contrast values of each ROI in three protocols.

4.6.1 MP-RAGE

In the analyses of cortical regions; according to independent samples t test results there is a significant difference in contrast between young and old participants. The mean contrast value of young volunteers is 0.198±0.053 and 0.107±0.033 for olds ($p \leq .01$). In subcortical structures, contrast decreased slightly but this difference is statistically meaningless. While the mean contrast in young participants is 0.143±0.020, the contrast in old subjects is 0.134±0.030. Overall, these contrast values are very low and contrast effects in subcortical regions results in a difficulty in differentiation of tissues. Furthermore, contrast of the aging population's MRIs are significantly lower than the young population, such a difference hinders good imaging of aging brains.

4.6.2 Spin Echo

In the aspect of cortical measurements, there is a noteworthy difference between young and old groups. The contrast in young group is 0.104±0.028; on the other hand old participants have a contrast value of 0.077±0.035 ($p \leq .003$). However, there is no statistically meaningful

difference between young and old subjects on the signal measure from subcortical regions. Compared to the MPRAGE contrasts, these contrast values are unacceptably low.

4.6.3 T_1 Estimated Images

The contrast value in young subjects that measured on cortical surface is 0.491±0.65, while the contrast in old participants showed a decrease, 0.368±0.118 but this difference is not significant. In subcortical area, contrast value in young group is 0.199±0.092 and as expected, a reduction in contrast value with increasing age was observed. Contrast in old group is 0.153±0.147 but the difference between two age groups is not statistically meaningful. Compared to the MPRAGE and SE protocols, the contrast values of T_1 estimated images using multi-spectral FLASH images fared better.

This might result in a great advantage in segmentation procedures and also in diagnosis.

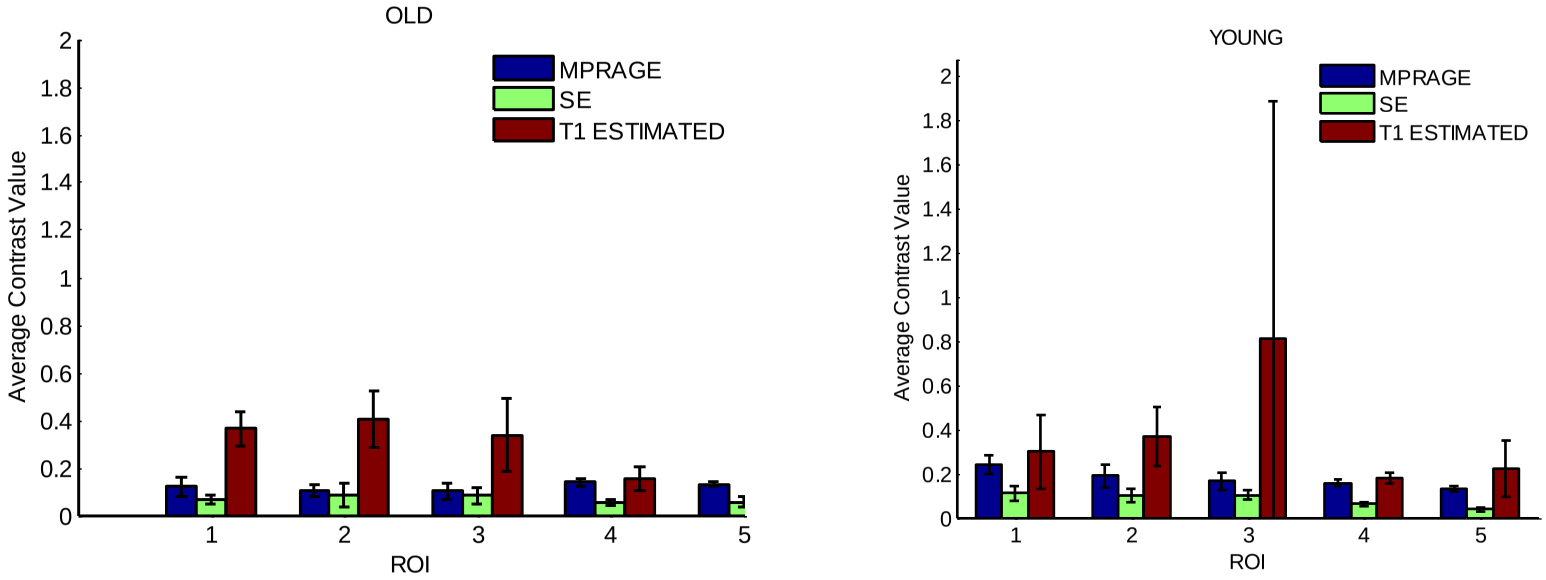

Figure 4.1 Average Contrast Values of each ROIs. 1: RMFG, 2: SFPC, 3: PCG, 4: Caudate, 5: Putamen.

4.7 Age Associated Changes in GWR

The combined graphs composed of GWR and contrast with increasing age can be seen on Figure 4.2. There is a difference between the GWR ranges of MPRAGE/SE images and T_1 estimated images. This difference happens because of the reversed intensity characteristics of the T_1 estimated images (i.e. CSF highest intensity, GM moderate intensity, WM lowest intensity). On the other hand, from the formulae in section 3, it is evident that GWR gets better as it gets farther away from the value 1. To accommodate range differences, graphs are generated by measuring the absolute distance of GWR from 1.

4.7.1 MP-RAGE

On cortical measures, Gray-White Ratio showed a significant increase in elderly participants indicating worse contrast. The GWR is 0.669±0.075 in young subjects and 0.804±0.054 in old ones which gives a significant difference between young and old participants. According to subcortical measurements, GWR exhibited statistically meaningless differences between these two age groups with the values is 0.748±0.030 in young group and 0.760±0.024 in older group. These GWR ratios are far from acceptable values.

4.7.2 Spin Echo

In cortical measurements, GWR demonstrated an important increase with aging ($p \leq .001$). The GWR in young volunteers is 0.809±0.045, whereas this ratio is 0.872±0.082 in elderly volunteers. Contrary to this significant difference there is no meaningful difference in subcortical level. GWR is 0.853±0.191 in young participants and 0.896±0.027 in old ones. The GWR of all landmarks were comparable worse than those of MPRAGE images, probably because of the inconvenience of this sequence to 3.0 T MRI scanners (Scarabino, 2003).

4.7.3 T_1 Estimated Images

The GWR measured on cortical landmarks is 2.453±0.818 for young participants and 2.315±0.649 for old ones. When considering subcortical areas, besides the smaller values than the cortical landmarks also there is no significant difference between young and old subjects. In the young subjects GWR is 1.367±0.311 and in older participants GWR is 1.340±0.184.

These values should be converted to the ranges of MPRAGE and SE for cross comparisons. In order to do that, we should look at the absolute difference of these values from 1.

As in contrast measurements, T_1 estimated images have the best GWR when compared to MPRAGE and SE.

In figures 4.3 and 4.4, GWR characteristics of the three imaging protocols are plotted against contrast separately for cortical and sub-cortical ROIs. As seen from here, T_1 estimated images have higher GWR and contrast values with respect to the others. In addition, young and old populations' characteristics are indistinguishable in T_1 estimated images. In other words, old population's images are not degraded in T_1 estimate images.

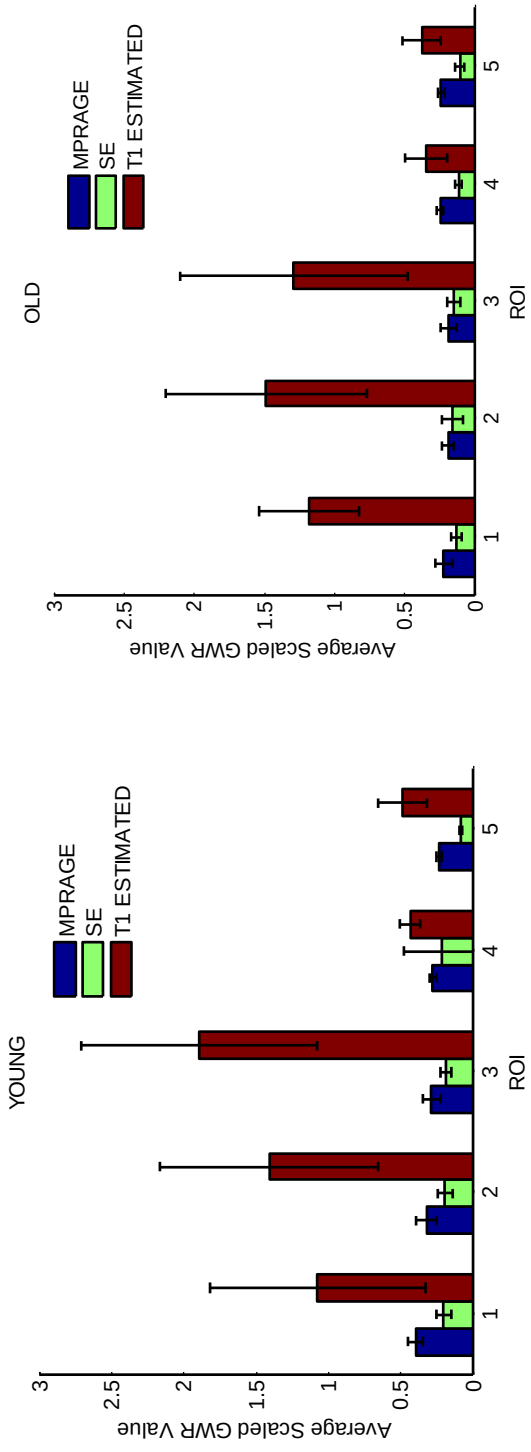

Figure 4.2 Average Scaled GWR Values of each ROIs. 1: RMFG, 2: SFPC, 3: PCG, 4: Caudate, 5: Putamen.

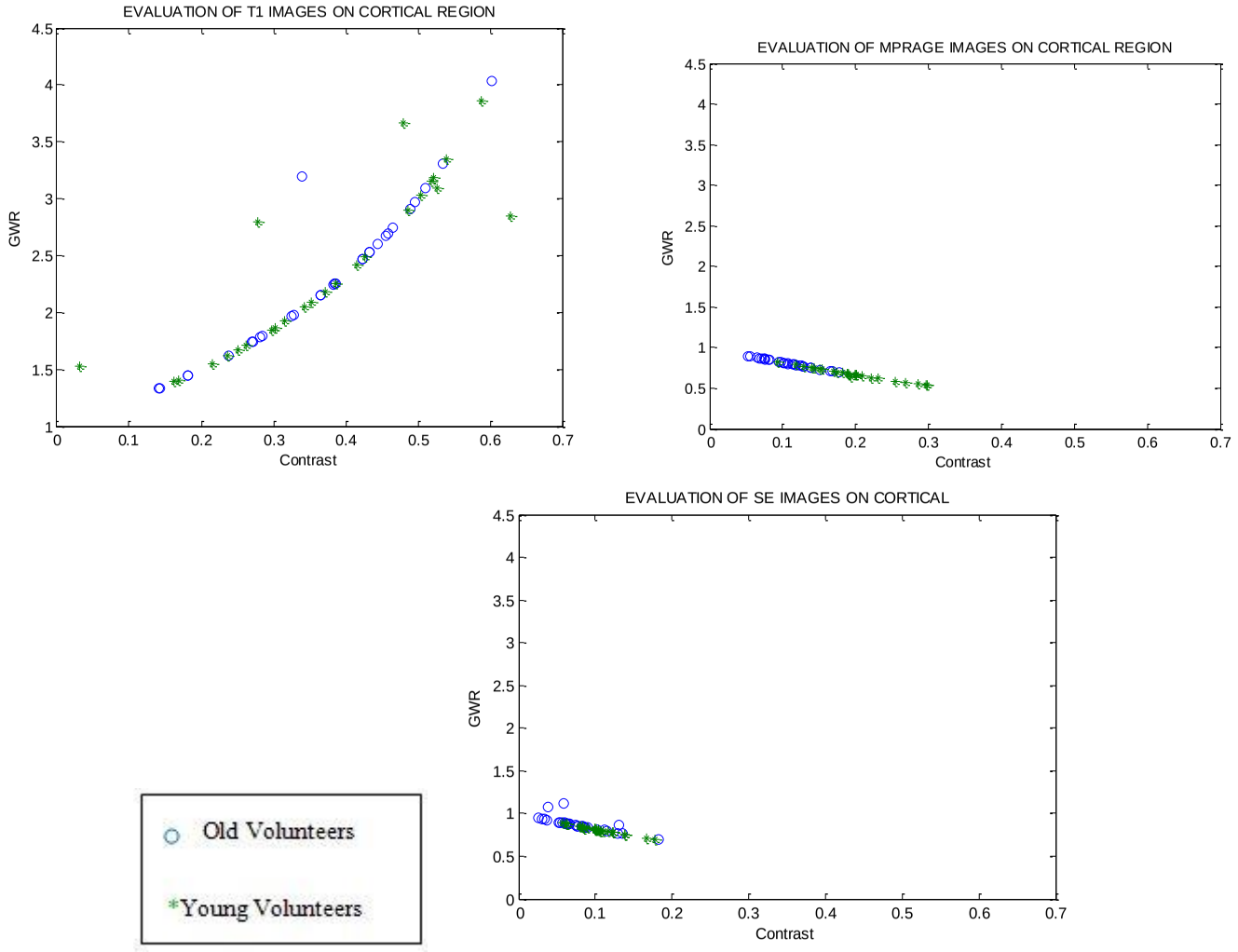

Figure 4.3 GWR-Contrast Graphs Distribution of SE, MPRAGE images behavior. and T_1 Estimated Images on cortical level.

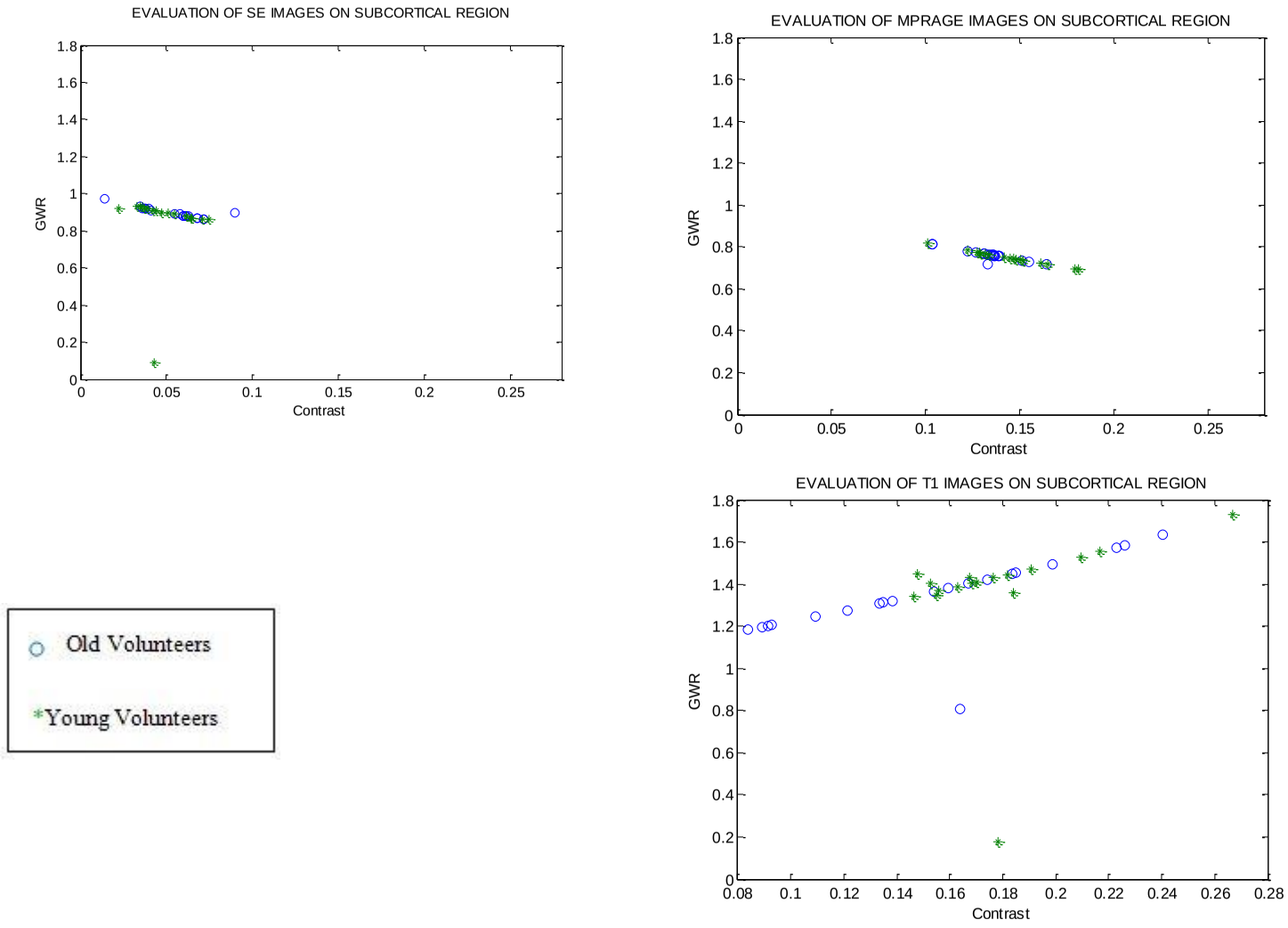

Figure 4.4 GWR-Contrast Graphs Distribution of SE, MPRAGE images behavior. and T_1 Estimated Images on

4.8 Effects of Age on SNR

The average SNR values of each ROI are shown in Figure 4.5.

4.8.1 MP-RAGE

SNR_{WM} measured on cortical landmarks showed marginally significant difference between young and old volunteers (p=.053). The SNR_{WM} in young group is 117.47±21.90 and in old ones is 104.46±27.08 with a mild reduction. SNR_{GM} is not significantly different between young and old individuals (SNR_{GM} is 79.20±18.16 in young participants and 84.22±22.05 in old ones).

In the analysis of SNR in subcortical landmarks, there are both significant differences between young and old groups for WM and GM. SNR_{WM} in young group is 143.86±16.73 and in older subjects SNR_{WM} is 123.98±13.60. SNR_{GM} is 109.98±15.66 in young volunteers and 94.19±9.51 in older ones. As reported in the literature, both SNR_{WM} and SNR_{GM} decreased with increasing age.

4.8.2 Spin Echo

SNR_{WM} and SNR_{GM} did not depict significant differences with aging on cortical level (SNR_{WM} is 193.66±81.43 in young volunteers and 170.73±69.73 in the elderly ones. SNR_{GM} is 157.54±68.92 in young participants while 148.34±60.42 in older participants). Similar to cortical measurements, SNR in subcortical landmarks showed statistically meaningless differences between age groups for WM and GM (SNR_{WM} in young group is 208.98±85.08 and in older subjects SNR_{WM} is 196.29±88.88. SNR_{GM} is 190.16±78.91 in young volunteers and 180.06±80.73 in older ones). Similar SNR characteristics for young and old populations are desirable. Furthermore, SNR characteristics of SE images are far better than those of MPRAGE. This might be due to the TR adjustment steps that we adopted during imaging.

4.8.3 T_1 Estimated Images

On cortical landmark evaluation, SNR_{WM} and SNR_{GM} gave statistically significant differences between young and old volunteers ($p \leq .001$). SNR_{WM} is 0.310±0.087 in young individuals, however 0.457±0.114 in older group. On the other hand, SNR_{GM} is 0.737±0.235 in young participants and 0.980±0.242 in old ones.

In subcortical level, to analyze SNR there is an unexpected outcome with significant higher SNR values in elderly individuals on both WM and GM landmarks ($p \leq .001$). SNR_{WM} is

0.555±0.049 in younger group and 0.690±0.125 for old ones. At the same time, SNR_{GM} is 0.788±0.066 for young subjects and 0.939±0.158 for old subjects.

Overall, the SNR characteristics of the T_1 estimated images are unacceptably low. This is due to the division by the standard deviation of the background area. Because of the computer algorithm that we used, T_1 estimates outside the brain are not a realistic procedure. Hence the divisor part in the SNR equation should be chosen from a more reliable ROI in the future.

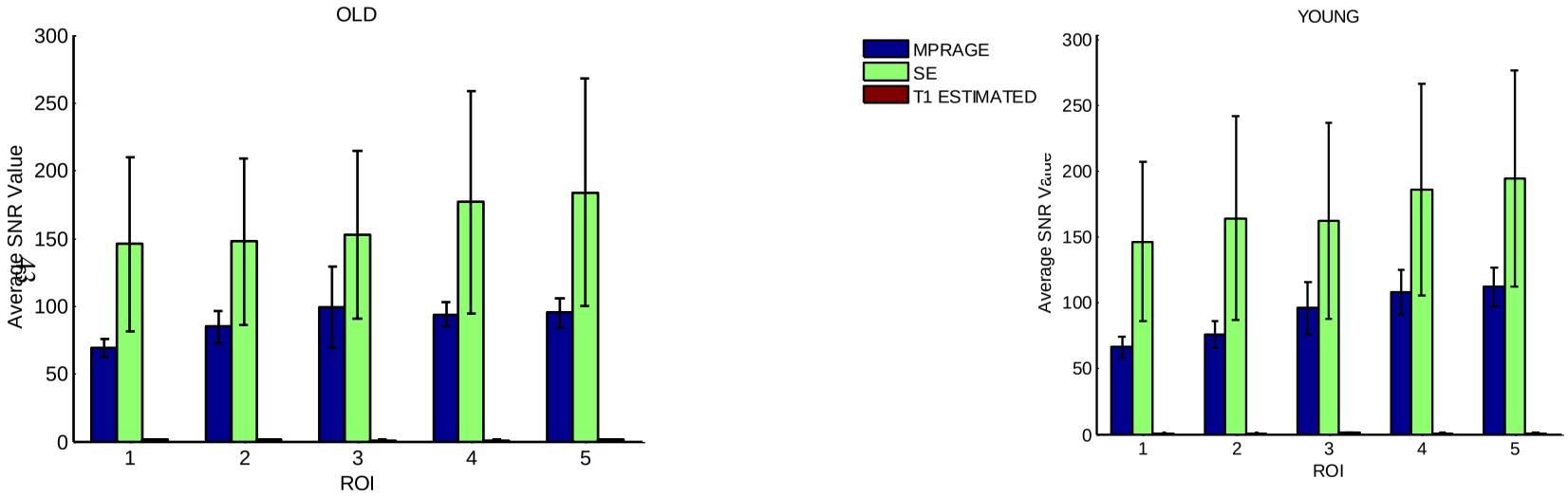

Figure 4.5 Average SNR Values of each ROIs. 1: RMFG, 2: SFPC, 3: PCG, 4: Caudate, 5: Putamen

4.9 Age Dependent Changes on CNR

The average CNR value of each ROI can be shown in Figure 4.6.

4.9.1 MP-RAGE

CNR in old volunteers was statistically different from young subjects and decreased with aging ($p \leq .001$) on cortical level. CNR in young group is 38.26±10.56 and in old group is 20.24±8.08.

On the other hand, CNR did not differ significantly with aging in the subcortical measurements. CNR value in young subjects is 33.87±7.49 and 29.78±5.22 in old subjects.

4.9.2 Spin Echo

The alteration in CNR with aging is significant on cortical measurements. CNR is calculated as 35.89±16.13 in young group and 24.20±16.26 in old subjects.

Unlike cortical computations, there is no meaningful change in CNR measured on subcortical level with increasing age. CNR measured on young group is 18.82±8.09 and on old group is 20.25±10.63.

The mean value of CNR in cortical regions acquired from MP-RAGE and SE images is really close to each other, but in terms of subcortical CNR, MPRAGE is inarguably better than SE.

4.9.3 T_1 Estimated Images

CNR measured on cortical landmarks and the resulting values; 0.491±0.65 for young subjects and 0.368±0.118 for old individuals. The difference in CNR with increasing age is not meaningful.

Resemble to cortical measures, CNR on subcortical level did not have a significant difference through age. CNR is 0.199±0.092 in young group and 0.153±0.047 in older group.

Similarly to SNR values, the CNR values of the T_1 estimated images are unacceptably low. This should be remedied in the future by changing the ROI from which noise is computed.

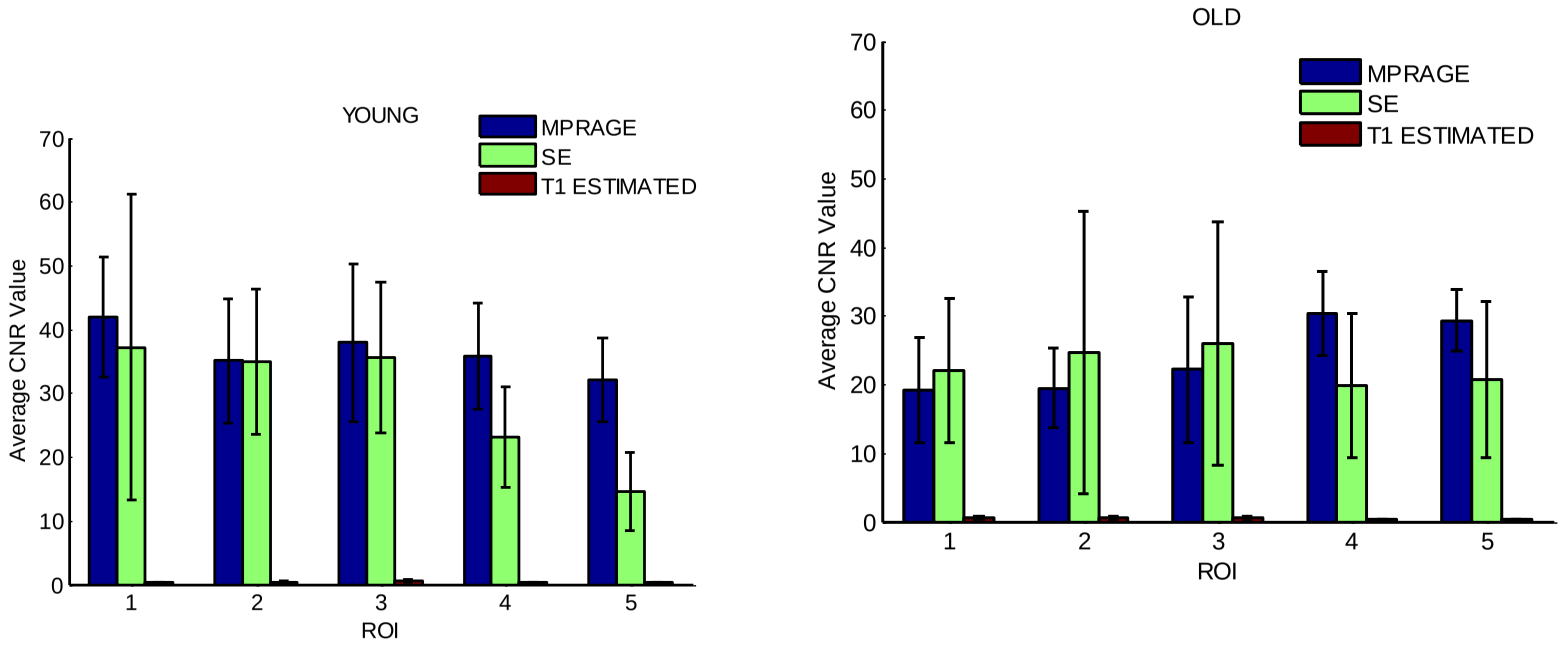

Figure 4.6 Average CNR Values of each ROIs. 1: RMFG, 2: SFPC, 3: PCG, 4: Caudate, 5: Putamen.

CHAPTER 5

DISCUSSION

It is expected that there will be contrast differences between young and old subjects in MPRAGE sequence and the contrast in old volunteers is lower than the young.

In MPRAGE analysis conducted on cortical areas, it is found that CNR and contrast decreased significantly with aging, GWR increased with increasing age and the reduction in SNR_{WM} is almost statistically meaningful in old volunteers, although SNR_{GM} did not show a significant difference between young and old subjects.

The signal measured on subcortical level demonstrated a significant reduction in SNR_{GM} and SNR_{WM}. However, the difference in contrast, GWR and CNR is not meaningful through young and old participants.

Cortical:

A study by Salat and colleagues (2009) examined age associated alterations in cortical gray and white matter signal intensity and gray to white matter contrast, demonstrating that there is a region dependent decrease in WM and GM intensity with age especially in medial frontal regions. Also in superior and anterior cingulum regions the WM signal decreases were the biggest. The age associated reduction in WM signal intensity is more prominent than GM and the areas of these two changes overlaid are also regionally specific (Salat, 2009; Gutmann, 1998; Resnick, 2003). This decrease in WM and GM signal intensities leads to a reduction in SNR and hence CNR values. Additionally, in aged individuals they found an increase in GWR towards to 1 indicating a degradation of contrast. Our findings can be considered as a replication of this study.

Lots of earlier studies conducted on aging also demonstrated that there is a reduction in differentiation GM and WM and a decreased contrast in aged population (Jernigan et al., 1991; Magnaldi et al., 1993; Raz et al., 1990). Also it is important to note that one of the possible reasons of this decrease might be that WM signal intensity gets more similar to GM intensity with increased age (Jernigan et al., 1991; Raz et al., 1990). Another alternative cause of these signal alterations might be attributed to specific myelination patterns that occur during aging

(Salat, 2009; Peters, 2002). The signal change is probably related to demyelination of WM and also the alterations of mineral, water (increase in water content) and protein content of the underlying tissue (Davatzikos, 2002; Wiggins, 1988). Furthermore, loss of dendritic arbors in GM may increase the GM signal, causing higher density of WM streaks within cortex.

Subcortical:

In a study conducted by Braffman et. al. (1988), the hyperintense deep white matter lesions mainly result from subtle alterations of gliosis and demyelination in 60 years and older subjects. There are lots of studies demonstrating white matter hyperintensities at subcortical level around the ventricles in elderly population, despite most of the alterations are subtle (Ylikoski, 1995; Christiansen, 1994; Wahlund, 1996; Sachdev, 2003; Fazekas, 1987). Age dependent subcortical alterations are less common than cortical alterations and have a prevalence of 20% (Sachdev, 2003).

We expect that the contrast of SE with adjusted TR is better than MPRAGE

When we compare SE and MPRAGE images, the expectation is partially satisfied with respect to SNR values: SE images have higher SNR than MPRAGE. However, this result is not valid for CNR measurements in which MPRAGE has higher CNR than SE. On the contrary to our expectations, MPRAGE has better contrast values and smaller GWR than SE.

The reason of low contrast on SE is likely because of the high magnetic field of the MRI scanner. Nobauer-Huhmann et. al. (2002) conducted a study on contrast enhancement of brain tumors on MR images and compared the results both at 3.0 T and 1.5 T. They evaluated the distinguishability of WM and GM on SE T_1 weighted images visually and found a significant reduction in contrast a 3.0 T. Also it was reported that TR optimized for 1.5 T was too long to acquire sufficient contrast at 3.0 T (Nobauer-Huhmann, 2002). There are different opinions existing in literature about GM and WM differentiation on SE T_1-weighted images at 3.0 T. Ideally, 3.0 T promises increased signal-to-noise ratio since magnetization increases as the square of the magnetic field strength while noise increases linearly twice of signal-to-noise ratio from 1.5 T to 3.0 T. However, in practice, 'this doubled signal-to-noise ratio is a myth' (Ross, 2004). Ruggieri et. al. (2002) reported that they had not been able to accomplish a decrease in overall imaging duration as a consequence of the prolonged T_1 relaxation at the 3.0 T and power deposition (Ruggieri, 2002). In order to have an acceptable distinction between GM and WM the usage of a T_1-weighted GE or an IR (Inversion Recovery) sequence is required because of longer T_1 relaxation time. The image contrast on T_1-weighted images is distorted by increased chemical shift artifact at 3.0 T than 1.5 T (Ross, 2004). There are lots of studies demonstrating a degraded contrast and CNR values at 3.0 T and the probable reason is longer relaxation times at 3.0 T (Scarabino, 2003; Sasaki, 2003; Ross, 2004; Isoda, 2010; Schmitsz, 2005). Additionally, Isoda et. al. (2010) reported that it was difficult to optimize T_1 weighted images to acquire both sufficient contrast and high spatial resolution at 3.0 T scanners. This contrast reduction in SE T_1

weighted images results in the opening of discussions about the appropriateness of these sequences at higher field strengths in routine clinical brain imaging (Schmitz, 2005; Ross, 2004).

Another possible explanation can be the partial volume effect. Due to scanner constraints the slice thickness of SE images is 3 mm hence the increasing of slice thickness introduces PVE and distorted signal measurements.

Cortical:

Fushimi et. al. (2007) compared gray matter and white matter contrast at 3.0 T and 1.5 T and reported that contrast to noise ratio is 8.61±2.55 in frontal lobe on MR images acquired at 3.0 T scanner. This value is really smaller than proposed method for optimizing contrast in SE sequence in this study.

This finding is important because there are lots of studies demonstrating low contrast on SE images at 3.0 T (Schmitz, 2005; Isoda, 2010; Lu, 2005).

Subcortical:

There are alterations in subcortical nuclei with increasing age and important influences on hippocampus, amygdala, thalamus, caudate, putamen and pallidum (Walhovd, 2005). In a study by Long et. al. (2012), it is demonstrated that the reduction in caudate nucleus is connected not only to successful aging but also neurologic disorders (Long, 2012; Jernigan, 2001; Corson, 1999). This might be one of the reasons of signal changes on caudate.

In a study, Lu and colleagues (2005) conducted the measurements of T_1 and T_2 relaxation times of 10 healthy participants on both 1.5 and 3.0 T and compared the results. In order to calculate MRI quality metrics they drew ROIs only at subcortical level (including caudate and putamen) and the way of calculation SNR was the same as in this study. The outcome of their experiment on 3.0 T for SNR_{WM} is 101.5±6.8 and SNR_{GM} is 81.1±4.9.

The difference in T_1 tissue values between young and old individuals should be significant, probably with a prolongation with aging.

According to our expectations, we expected significant T_1 differences between young and aged subjects which are satisfied in contrast and GWR measurements. Except for Posterior Central Gyrus, T_1 values measured on all of the landmarks showed an increase with aging.

Deichmann et. al. (1999) developed a method to acquire fast T_1 mapping using a series of FLASH images and found T_1 WM as 676 ± 6 ms and T_1 GM as 1223 ± 22. Our study replicates similar measures: average T_1 value of 9 healthy young subject is 605.75 msec for WM and 1147.2 msec for GM . Yet another study demonstrated that spin-lattice relaxation time of GM is 1109±18 msec and WM is 565 ± 7msec that is coherent with our results (Steinhoff, 2001). In addition, Gelman and colleagues (2001) analyzed longitudinal relaxation rates in human brain

($R_1=1/T_1$) and found that T_1 of caudate head is 1483 ± 42msec, putamen 1337±42ms, globus pallidus 1043 ± 37msec whereas frontal WM is 847 ± 43msec.

Similarly, Wansapura et. al. (1999) conducted a study about NMR relaxation times at 3.0 T evaluating on 19 healthy normal subjects and reported that average T_1 values measured for gray matter and white matter were 1331 and 832 msec, respectively.

It is important to note that relaxation times vary depending on magnetic field strength and T_1 relaxation time is 14% to 30% longer at 3.0 T then compared to the outcomes of 1.5 T (Lu, 2005).

Better contrast on T_1 estimated images is expected compared to MPRAGE and SE, especially on subcortical areas.

This is an important expectation which is satisfied in this thesis work. The contrast and GWR calculated on T_1 estimated images are inarguably than the ones in MPRAGE and SE.

For example, in a recent study, Traynor et. al (2011) developed a method based on an anatomical hypothesis established previously and T_1/T_2 values in order to segment the human thalamus and they reported that the outcome of a segmentation process based on relaxation times gives more reliable results.

5.1 Future Work

The SE sequence showed worse contrast compared to other sequences. There are several studies indicating that SE sequence at 3.0 T performs worse than SE at 1.5 T (Scarabino, 2003; Sasaki, 2003; Ross, 2004; Isoda, 2010; Schmitsz, 2005). Conducting a comparison study at 1.5T may reveal different results in terms of the signal characteristics of SE.

The SNR of GM and WM in MPRAGE/SE images are out of scale with respect to that of T_1 estimations. This is because the background area on the T_1 estimated images are extremely noisy. Although the contrast and GWR values of the T_1 estimated images are more acceptable that those of MPRAGE and SE, calculation of SNR using a different metric should be performed in the future.

Finally, the comparison of the MPRAGE, SE and T_1 estimated images based on age and contrast characteristics can be performed via a clustering algorithm.

CHAPTER 6

CONCLUSION

The detection and comparison of the changes in brain as a result of healthy aging or a neurological disease is a difficult process considering the wealth of variation in MRI sequences, scanners, technical properties and the resulting artifacts. Instead of using tissue signal intensities, usage of intrinsic tissue parameters such as spin-lattice relaxation time which is the principle origin of the tissue contrast in MR images promises a more valid metric.

Although there are a large number of studies that measure morphological changes in aging brains, there is a limited number of studies examining how the signal characteristics of different brain tissues are affected by normal or pathological aging. The characterization of signal changes with healthy aging or disease provides important information that is complementary to morphometric studies of regional brain volumes (Davatzikos, 2002). Within this concept, this thesis work exhibits importance since it is composed of signal variations acquired from different MRI sequences and T_1 mapped images in aging brains.

The MRI scans were conducted on 19 neurologically healthy subjects (10 old, 9 young) and MPRAGE, SE and multi-spectral FLASH acquisitions of the same participant is gathered in the same session. Later on the T_1 estimated images were created offline in the laboratory environment. 5 different ROIs for GM and 4 ROIs for WM were traced on 3 images: MPRAGE, SE; T1 estimated image. Then image quality measurements were performed via contrast, GWR, SNR and CNR calculations. The independent samples t-test was utilized for the analysis of these parameters in young and old participants.

Results obtained in the current study are summarized as follows:

In the MPRAGE images, the signal measured on cortical area showed a significant difference between young and old participants with a decrease in contrast and CNR but with an increase in GWR in old participants. This indicates degraded image qualities in the aging population. SNR calculations did not have a significant difference between two age groups. Although, at subcortical level, CNR, contrast and GWR did not depict a meaningful difference with aging, SNR calculated for GM and WM showed a significant with increasing age.

In the evaluation of SE images, CNR and contrast reduced and GWR increased significantly and SNR did not show a significant difference with aging like MPRAGE on cortical regions. Nevertheless, none of the parameters demonstrated a significant difference between old and young subjects in subcortical measurements.

In cortical areas on T_1 estimated images, SNR_{GM} SNR_{WM} showed a significant increase with aging but the other factors did not have a meaningful difference between old and young subjects. The signals obtained in subcortical areas showed the same behavior as cortical measurements in T_1 estimated images.

In the analyses of spin-lattice relaxation time (T_1) alterations between young and old individuals in specific ROI base; Caudate, putamen, caudate-putamen adjacent WM, rostral middle frontal gyrus (RMFG), rostral middle frontal gyrus adjacent WM (RMFG_WM) and the crossing point of superior frontal sulcus and pre-central sulcus (SFPC) showed a significant increase with aging. The alterations in SFPC_WM, PCG and PCG_WM were not significant. The contrast and GWR metrics were the best in all of these three MRI sequences.

Overall, the best SNR was obtained in SE images probably due to our TR adjustment scheme, and the highest results in CNR was observed in SE and MPRAGE images with subtle differences. It is important to mention that the T_1 estimated images return somewhat arbitrary noise results when the ROI to depict noise is retrieved from the background area. Probably due to this, SNR and CNR values in T_1 estimated images were extremely low (i.e. noise was high). In the future, a better ROI for depicting noise levels of T_1 estimated images will be utilized.

As we hoped for, the highest contrast values and best GWR were observed in T_1 estimated images. Furthermore, age-related contrast and GWR differences were not observable in T_1 estimated images, which is a feature sought after in high quality imaging. We believe that our study provides important validation guidelines for imaging protocols in healthy aging.

REFERENCES

Bernstein MA, King KF, Zhou ZJ. Handbook of MRI pulse sequences. Burlington, Mass: Elsevier, 2004.

Blatter, Duane D., et al. "Quantitative volumetric analysis of brain MR: normative database spanning 5 decades of life." *American journal of Neuroradiology* 16.2 (1995): 241-251.

Braffman, B. H., et al. "Brain MR: pathologic correlation with gross and histopathology. 2. Hyperintense white-matter foci in the elderly." *American Journal of Roentgenology* 151.3 (1988): 559-566.

BrainWeb: Simulated Brain Database, http://brainweb.bic.mni.mcgill.ca/brainweb/, 09/01/2013. 1:48 pm.

Brody H. Structural changes in the aging nervous system. *Interdiscip Topics Gerontol*. 1970; 7:9–21.

Buxton, R.B, Introduction to Functional Magnetic Resonance Imaging, Cambridge University Press, 2002

Cho S, Jones D, Reddick WE, Ogg RJ and Steen RG, Establishing norms for age related changes in proton T1 of human brain tissue in vivo. Magnetic Resonance Imaging, Vol. 15, No. 10, pp. 1133-l 143, 1997

Christiansen P, Larsson HBW, Thomsen C, Wieslander SB, Henriksen O. Age dependent white matter lesions and brain volume changes in healthy volunteers. *Acta Radiol*. 1994; 35:117–122.

Coffey CE, Lucke JF, Saxton JA, Ratcliff G, Unitas LJ, Billig B, Bryan RN, Sex Differences in Brain Aging A Quantitative Magnetic Resonance Imaging Study, *Arch Neurol*. 1998;55(2):169-179

Coffey CE, Wilkinson WE, Parashos IA, Soady SA, Sullivan RJ, Patterson LJ, Figiel GS, Webb MC, Spritzer CE, Djang WT. Quantitative cerebral anatomy of the aging human brain; a cross-sectional study using magnetic resonance imaging. *Neurology.* 1992; 42:527–536.

Coleman, Paul D., and Dorothy G. Flood. "Neuron numbers and dendritic extent in normal aging and Alzheimer's disease." *Neurobiology of aging* 8.6 (1987): 521-545.

Convit A, De Leon MJ, Tarshish C, De Santi S, Tsui W, Rusinek H and George A, Specific Hippocampal Volume Reductions in Individuals at Risk for Alzheimer's Disease, Neurobiology of Aging, Vol. 18, No. 2, pp. 131–138, 1997

Corson PW, Nopoulos P, Andreasen NC, et al. Caudate size in firstepisode neuroleptic-naive schizophrenic patients measured using an artificial neural network. Biol Psychiatry 1999; 46:712–720.

Courchesne E, Chisum HJ, Townsend J, Cowles A, Covington J, Egaas B, Harwood M, Hinds S, Press GA, Normal Brain Development and Aging: Quantitative Analysis at in Vivo MR Imaging in HealthyVolunteers, Radiology 2000; 216:672-682

Cox RW (1996): AFNI, software for analysis and visualization of functional magnetic resonance neuroimages. Comput Biomed Res 29:162–173.

Davatzikos C, Resnick SM (2002) Degenerative age changes in white matter connectivity visualized *in vivo* using magnetic resonance imaging. Cereb Cortex 12:767–771

Davis T A, Sigmon K, Matlab Primer Seventh Edition. A CRC Press Company Boca Raton London New York Washington, D.C. 2005.

Deichmann R, Good C D, Josephs O. *Optimization of 3-D MP-RAGE Sequences for Structural Brain Imaging.* NeuroImage 12, 112-127, 2000.

Deichmann, R., D. Hahn, and A. Haase. "Fast T1 mapping on a whole-body scanner." *Magnetic resonance in medicine* 42.1 (1999): 206-209.

Dekaban AS, Sadowsky D. Changes in brain weights during the span of human life: relation of brain

Dickerson BC, Bakkour A, Salat DH, Feczko E, Pacheco J, Greve DN, Grodstein F, Wright CI, Blacker D, Rosas HD, Sperling RA, Atri A, Growdon JH, Hyman BT, Morris JC, Fischl B, Buckner RL. The Cortical Signature of Alzheimer's Disease: Regionally Specific Cortical Thinning Relates to Symptom Severity in Very Mild to Mild AD Dementia and is Detectable in Asymptomatic Amyloid-Positive Individuals. Cereb Cortex. 2008

Donald W. McRobbie, Elizabeth A. Moore, Martin J. Graves, Mertin R. Prince (2003). *MRI From Picture to Proton*. Second edition (2007). New York: Cambridge University Press. ISBN: 10 0-521-68384-x.

Driscoll I, Davatzikos I, An Y, Wu X, Shen D, Kraut M, Resnick SM, Longitudinal pattern of regional brain volume change differentiates normal aging from MCI, Neurology 72 June 2, 2009, vol. 72 no. 22 1906-1913

Ertan T, Eker E, Şar V: Reliability, validity and factor structure of the geriatric depression scale in Turkish elderly: are there different factor structures for different cultures? Int Psychogeriatr 2000; 12:163-172.

Fazekas, Franz, et al. "MR signal abnormalities at 1.5 T in Alzheimer's dementia and normal aging." *American Journal of Roentgenology* 149.2 (1987): 351-356.

Fischl B, Salat DH, van der Kouwe A.J., Makris N, Ségonne F, Quinn BT, Dale AM.,Sequence-independent segmentation of magnetic resonance images, NeuroImage 23 (2004) S69–S84

Fischl B, Salat DH, van der Kouwe AJ, et al. Sequence-independent segmentation of magnetic resonance images. Neuroimage 2004; 23(suppl 1):S69–S84.

Fushimi, Yasutaka, et al. "Gray matter-white matter contrast on spin-echo T1-weighted images at 3 T and 1.5 T: a quantitative comparison study." *European radiology* 17.11 (2007): 2921-2925.

Ge Y, Grossman RI, Babb JS, Rabin ML, Mannon LJand Kolson DL, Age-related total gray and white matter changes in normal adult brain. Part I: volumetric MR imaging analysis. AJNR AM J Neuroradiol 23;1327-1333, September 2002.

Gelman, Neil, et al. "Interregional variation of longitudinal relaxation rates in human brain at 3.0 T: relation to estimated iron and water contents." *Magnetic resonance in medicine* 45.1 (2001): 71-79.

George, D. (2003). SPSS for Windows Step by Step: A Simple Study Guide and Reference, 17.0 Update, 10/e. Pearson Education India.

Giannakopoulos, Panteleimon, et al. "Distinct patterns of neuronal loss and Alzheimer's disease lesion distribution in elderly individuals older than 90 years." *Journal of Neuropathology & Experimental Neurology* 55.12 (1996): 1210-1220.

Gökçay, D. (2009). 'Beyin Dokularının Bölütlenmesi: Yöntemlerin Sınıflandırılması, Zorluklar, Yeni Yaklaşımlar', In: M. Özgören, A. Öniz (Eds.), The Applied Biophysics-Uygulamali Beyin Biyofizigi ve Multidisipliner Yaklasim-(pp. 111-132). Izmir, Turkey: Dokuz Eylul Yayinlari, D.E.U. Rektorluk Matbaasi (ISBN 978-975-441-259-8)

Gökçay D, Summary of estimation of T1 relaxation times from a given set of FLASH images, Technical Report, University of California San Diego, Laboratory for Research on the Neuroscience of Autism, 2004

Gold S, Christian B, Arndt S, Zeien G, Cizadlo T, Johnson D L, Flaum M, and Andreasen N C. Functional MRI statistical software packages: a comparative analysis. Human Brain Mapping, 6:73-84, 1998.

Gómez-Isla, Teresa, et al. "Neuronal loss correlates with but exceeds neurofibrillary tangles in Alzheimer's disease." *Annals of neurology* 41.1 (1997): 17-24.

Gómez-Isla, Teresa, et al. "Profound loss of layer II entorhinal cortex neurons occurs in very mild Alzheimer's disease." The Journal of neuroscience 16.14 (1996): 4491-4500.

Guttmann CR, Jolesz FA, Kikinis R, et al. White matter changes with normal aging. Neurology 1998; 50:972–978.

Harper CG, Kril JJ, Holloway RL. Brain shrinkage in chronic alcoholics — a pathological study. *Br Med J*. 1985; 290:501–504.

Heiken J P, Manual of the Clinical Magnetic Resonance Imaging. Editted by Brown J J. Raven Press, New York,1991.

Hendrick, R. E. Image contrast and noise. In *Magnetic resonance imaging,* Vol. 1, edited by D. D. Stark and W. G. Bradley, pp. 43-67. St. Louis, MO: Mosby. 1999.

Ho K, Roessmann U, Straunfjord JV, Monroe G. Analysis of brain weight. I. Adult brain weight in relation to sex, race, and age. *Arch Path Lab Med*. 1980; 104:635–639.

Isoda, Hiroyoshi, et al. "Contrast behavior of high-spatial-resolution T1-weighted MR imaging at 3.0 T vs. 1.5 T." *Clinical Imaging* 35.2 (2011): 133-138.

Jenkinson M, Beckmann C F, Behrens T E, Woolrich M W, Smith S M. FSL. NeuroImage, Volume 62, Issue 2, 15 August 2012, Pages 782-790.

Jernigan TL, Archibald SL, Berhow MT, Sowell ER, Foster DS, Hesselink JR. Cerebral structure on MRI, Part I: Localization of age-related changes. Biol Psychiatry 1991;29:55–67. [PubMed: 2001446]

Jernigan TL, Archibald SL, Fennema-Notestine C, et al. Effects of age on tissues and regions of the cerebrum and cerebellum. Neurobiol Aging 2001; 22:581–594.

Kril JJ, Halliday GM. Brain shrinkage in alcoholics: a decade on and what have we learned? *Prog Neurobiol*. 1999; 58:381–387.

Lee, Hak Sik, and Ji Hoon Lee. "SPSS 17.0 Manual." *Seoul: Bob Mun Sa*(2009).

Liu, Junjie V., Nicholas A. Bock, and Afonso C. Silva. "Rapid high-resolution three-dimensional mapping of T< sub> 1</sub> and age-dependent variations in the non-human primate brain using magnetization-prepared rapid gradient-echo (MPRAGE) sequence." *NeuroImage* 56.3 (2011): 1154-1163.

Long, X., Liao, W., Jiang, C., Liang, D., Qiu, B., & Zhang, L. (2012). Healthy aging: an automatic analysis of global and regional morphological alterations of human brain. *Academic Radiology*, *19*(7), 785-793.

Lu, Hanzhang, et al. "Routine clinical brain MRI sequences for use at 3.0 Tesla." *Journal of Magnetic Resonance Imaging* 22.1 (2005): 13-22.

Magnotta VA, Andreason NA, Schultz SK, Harris G, Cizadlo T, Heckel D, Nopoulos P, Flaum M. Quantitative in vivo measurement of gyrification in the human brain: changes associated with aging. *Cereb Cortex*. 1999; 9:151–160.

MATLAB, User's Guide, The MathWorks, Inc., Natick, MA 01760, 1992.

Moler C, MATLAB Users' Guide, Department of Computer Science University of New Mexico, 1980.

Moler, Cleve. "Matlab user's guide." *Alberquerque, USA* (1980).

MRIcro, http://www.mccauslandcenter.sc.edu/mricro/, last visited 17.08.2013

Mueller EA, Moore MM, Kerr DCR, Sexton G, Camicioli RM, Howieson DB, Quinn JF, Kaye JA. 1998. Brain volume preserved in healthy elderly through the eleventh decade. Neurology 51(6):1555--1562.

Murphy DG, de Carli C, Schapiro MB, Rapoport SI, Horwitz B. Age-related differences in volumes of subcortical nuclei, brain matter and cerebrospinal fluid in heathly men as measured with magnetic resonance imaging. *Arch Neurol*. 1992; 49:839–845.

Murphy DGM, DeCarli C, McIntosh AR, Daly E, Mentis MJ, Pietrini P, Szczepanik J, Schapiro MB, Grady CL, Horwitz B, Rapoport SI. 1996. Sex differences in human brain morphometry and metabolism: an in vivo quantitative magnetic resonance imaging and positron emission tomography study on the effect of aging. Arch Gen Psychiatry 53(7):585--594.

NeuroLex, http://neurolex.org, Last visited 26.08.2013.

Peters A. The effects of normal aging on myelin and nerve fibers: a review. J Neurocytol 2002; 31:581–593.

Raz N, Gunning FM, Head D, Dupuis JH, McQuain J, Briggs SD, Loken WJ, Thornton AE and Acker JD, Selective Aging of the Human Cerebral Cortex Observed *in Vivo*: Differential Vulnerability of the Prefrontal Gray Matter, Cerebral Cortex Apr/May 1997;7:268–282; 1047–3211/97

Resnick SM, Goldszal AF, Davatzikos C, Golski S, Kraut MA, Metter EJ, Bryan RN, Zonderman AB. One-year age changes in MRI brain volumes in older adults. Cereb Cortex 2000;10:464–472. 16

Resnick SM, Pham DL, Kraut MA, Zonderman AB and Davatzikos C,Longitudinal Magnetic Resonance Imaging Studies of Older Adults: A Shrinking Brain, The Journal of Neuroscience, April 15, 2003 • 23(8):3295–3301

Rettmann ME, Kraut MA, Prince J and Resnick SM, Cross-sectional and longitudinal analysis of anatomical sulcal changes associated with aging. Cerebral Cortex November 2006;16:1584-1594.

Robert W C, AFNI: What a long strange trip it's been. NeuroImage, 2011.

Rorden, C. "MRIcro—Medical Image viewer." (2002).

Rosen B, Wald L, (2006) Magnetic Resonance Analytic, Biochemical and Imaging Techniques, [Course notes], Massachusetts Institute of Technology: MIT OpenCourseWare. http://ocw.mit.edu, Last visited on 26.08.2013.

Ross, Jeffrey S. "The high-field-strength curmudgeon." *American journal of neuroradiology* 25.2 (2004): 168-169.

Ruggieri, P. M., et al. "Routine clinical imaging at 3.0 T: An oxymoron?."*Radiology*. Vol. 225. 820 JORIE BLVD, OAK BROOK, IL 60523 USA: RADIOLOGICAL SOC NORTH AMERICA, 2002.

S.M. Smith. Fast robust automated brain extraction. Human Brain Mapping, 17(3):143-155, November 2002.

Sachdev PS (Editted), The Ageing Brain: The Neurobiology and Neuropsychiatry of Ageing. Published bySwets & Zeitlinger Publishers, 2003, 49-60.

Salat DH, Buckner RL, Snyder AZ, Greve DN, Desikan RS, Busa E, Morris JC, Dale AM, and Fischl B. (2004). Thinning of the cerebral cortex in aging. Cereb. Cortex *14*, 721–730.

Salat DH, Kaye JA, and Janowsky JS, Prefrontal gray and and white matter volumes in healthy aging and Alzheimer disease. Arch. Neurol.1999, *56*, 338–344.

Salat DH, Lee SY, van der Kouwe AJ, Greve DN, Fischl B, Rosas HD, Age-associated alterations in cortical gray and white matter signal intensity and gray to white matter contrast. Neuroimage 2009;48:21-28.

Samorajski T. How the human brain responds to aging. *J Am Geriatr Soc*. 1976; 24:4–11.

Scarabino, Tommaso, et al. "3.0 T magnetic resonance in neuroradiology."*European journal of radiology* 48.2 (2003): 154-164.

Schmitz, Bernd L., et al. "Enhancing gray-to-white matter contrast in 3T T1 spin-echo brain scans by optimizing flip angle." *American journal of neuroradiology* 26.8 (2005): 2000-2004.

Sintorn, I-M., et al. "Gradient based intensity normalization." Journal of Microscopy 240.3 (2010): 249-258.

Smith S M, *Fast Robust Automated Brain Extraction.* Human Brain Mapping. 2002, 17:143-155.

Smith S.M., Jenkinson M., Woolrich M.W. Beckmann C.F., et al. (2004). *Advances in functional and structural MR image analysis and implementation as FSL.* NeuroImage 23 S208-S219.

SPSS Inc. Released 2008. SPSS Statistics for Windows, Version 17.0. Chicago: SPSS Inc.

Stanisz, Greg J., et al. "T1, T2 relaxation and magnetization transfer in tissue at 3T." *Magnetic Resonance in Medicine* 54.3 (2005): 507-512.

Steinhoff, S., et al. "Fast T1 mapping with volume coverage." *Magnetic resonance in medicine* 46.1 (2001): 131-140.

Stout, Julie C., et al. "Association of dementia severity with cortical gray matter and abnormal white matter volumes in dementia of the Alzheimer type."*Archives of neurology* 53.8 (1996): 742.

Sullivan EV, Marsh L, Mathalon DH, Lima KO, Pfefferbaum A. 1995. Age-related decline in MRI volumes of temporal lobe gray matter but not hippocampus. Neurobiol Aging 16(4):591--606.

Tang, Y., Nyengaard, J. R., Pakkenberg, B., & Gundersen, H. J. G. (1997). Age-induced white matter changes in the human brain: a stereological investigation. *Neurobiology of aging*, *18*(6), 609-615.

Thambisetty M, Wan J, Carass A et al., Longitudinal changes in cortical thickness associated with normal aging. Neuroimage 2010; 52:1215-1223.

Traynor, Catherine R., et al. "Segmentation of the thalamus in MRI based on T1 and T2." *NeuroImage* 56.3 (2011): 939-950.

Wahlund LO, Almkvist O, Basun H, Julin P. MRI in successful aging, a five year follow-up study form the eighth to the ninth decade of life. *Mag Reson Imaging*. 1996; 14:601–608.

Walhovd K, Fjell A, Reinvang I, et al. Effects of age on volumes of cortex, white matter and subcortical structures. Neurobiol Aging 2005; 26: 1261–1270.

Wallisch P, Lusignan M, Benayoun M, Baker T I, Dickey A S, Hatsapoulos N G. Matlab for Neuroscientists. An introduction to Scientific Computing in Matlab. Academic Press is an imprint of Elsevier, pp. 7-8, 2009.

Wansapura, Janaka P., et al. "NMR relaxation times in the human brain at 3.0 tesla." *Journal of magnetic resonance imaging* 9.4 (1999): 531-538.

Wiggins, Richard C., et al. "Effects of aging and alcohol on the biochemical composition of histologically normal human brain." *Metabolic brain disease* 3.1 (1988): 67-80.

Xu J, Kobayashi S, Yamaguchi S, Iijima K, Okada K, Yamashita K. Gender effects on age related changes in brain structure. *Am J Neuroradiol*. 2000; 21: 112–118.

Ylikoski, Ari, et al. "White matter hyperintensities on MRI in the neurologically nondiseased elderly Analysis of cohorts of consecutive subjects aged 55 to 85 years living at home." *Stroke* 26.7 (1995): 1171-1177.

Yongyue Zhang, Michal Brady, Stephen Smith (2001). *Segmentation of Brain MR Images Through a Hidden Markov Random Field Model and the Expectation-Maximization Algorithm*. IEEE. Transactions on Medical Imaging vol. 20, no. 1.

Yue NC, Arnold AM, Longstreth Jr. WT, Elster AD, Jungreis CA, O'Leary DH, Poirier VC, Bryan RN. Sulcal, Ventricular and white matter changes at MR imaging in the aging brain: data from the cardiovascular health study. *Radiology*. 1997; 202:33–39.

Yue NC, Arnold AM, Longstreth WT Jr, Elster AD, Jungreis CA, O'Leary DH, Poirier VC, Bryan RN. Sulcal, ventricular, and white matter changes at MR imaging in the aging brain: data from the cardiovascular health study. *Radiology*. 1997; 202:33–39.

Zhang, Y. and Brady, M. and Smith, S. Segmentation of brain MR images through a hidden Markov random field model and the expectation-maximization algorithm. IEEE Trans Med Imag, 20(1):45-57, 2001.

Ziegler DA, Piguet O, Salat DH, Prince K, Connally E, Corkin S, Cognition in healthy aging is related to regional white matter integrity, but not cortical thickness, Neurobiology of Aging 31 (2010) 1912–1926.

APPENDIX A

GERIATRIC DEPRESSION SCALE

Ad Soyad: .....

Toplam Puan: .....

Lütfen yaşamınızın son bir haftasında kendinizi nasıl hissettiğinize ilişkin aşağıdaki sorularda uygun olan yanıtı daire içine alınız.

1) Yaşamınızdan temelde memnun musunuz?

Evet Hayır

2) Kişisel etkinlik ve ilgi alanlarınızın çoğunu halen sürdürüyor musunuz ?

Evet Hayır

3)Yaşamınızın bomboş olduğunu hissediyor musunuz?

Evet Hayır

4) Sık sık canınız sıkılır mı?

Evet Hayır

5) Gelecekten umutsuz musunuz?

Evet Hayır

6) Kafanızdan atamadığınız düşünceler nedeniyle rahatsızlık duyduğunuz olur mu?

Evet Hayır

7) Genellikle keyfiniz yerinde midir?

Evet Hayır

8) Başınıza kötü birşey geleceğinden korkuyor musunuz?

Evet Hayır

9) Çoğunlukla kendinizi mutlu hissediyor musunuz?

Evet Hayır

10) Sık sık kendinizi çaresiz hissediyor musunuz?

Evet Hayır

11) Sık sık huzursuz ve yerinde duramayan biri olur musunuz?

Evet Hayır

12) Dışarıya çıkıp yeni birşeyler yapmaktansa, evde kalmayı tercih eder misiniz?

Evet Hayır

13) Sıklıkla gelecekten endişe duyuyor musunuz?

Evet Hayır

14) Hafızanızın çoğu kişiden zayıf olduğunu hissediyor musunuz?

Evet Hayır

15) Sizce şu anda yaşıyor olmak çok güzel bir şey midir?

Evet Hayır

16) Kendinizi sıklıkla kederli ve hüzünlü hissediyor musunuz?

Evet Hayır

17) Kendinizi şu andaki halinizle değersiz hissediyor musunuz?

Evet Hayır

18) Geçmişle ilgili olarak çokça üzülüyor musunuz?

Evet Hayır

19) Yaşamı zevk ve heyecan verici buluyor musunuz?

Evet Hayır

20) Yeni projelere başlamak sizin için zor mudur?

Evet Hayır

21) Kendinizi enerji dolu hissediyor musunuz?

Evet Hayır

22) Çözümsüz bir durum içinde bulunduğunuzu düşünüyor musunuz?

Evet Hayır

23) Çoğu kişinin sizden daha iyi durumda olduğunu düşünüyor musunuz?

Evet Hayır

24) Sık sık küçük şeylerden dolayı üzülür müsünüz?

Evet Hayır

25) Sık sık kendinizi ağlayacakmış gibi hisseder misiniz?

Evet Hayır

26) Dikkatinizi toplamakta güçlük çekiyor musunuz?

Evet Hayır

27) Sabahları güne başlamak hoşunuza gidiyor mu?

Evet Hayır

28) Sosyal toplantılara katılmaktan kaçınır mısınız?

Evet Hayır

29) Karar vermek sizin için kolay oluyor mu?

Evet Hayır

30) Zihniniz eskiden olduğu kadar berrak mıdır?

Evet Hayır

APPENDIX B

TR ADJUSTMENT

Given M_x and M_z in the SE sequence:

$$M_x(t) = M_x(0)e^{-\frac{t}{T_2}}$$

$$M_z(t) = M_o\left(1 - e^{-\frac{t}{T_1}}\right) + M_z(0)e^{-\frac{t}{T_1}}$$

$M_x(0) = 0;$ $\quad M_z(0) = M_o$

$M_x(1) = M_o$ $\quad M_z(1) = 0$

$M_x(2) = 0$ $\quad M_z(2) = M_o\left(1 - e^{-\frac{TR}{T_1}}\right)$

$M_x(3) = M_z(2) = M_o\left(1 - e^{-\frac{TR}{T_1}}\right)$ $\quad M_z(3) = 0$

$M_x(4) = 0$ $\quad M_z(4) = M_o\left(1 - e^{-\frac{TR}{T_1}}\right)$

$M_x(5) = M_z(4) = M_o\left(1 - e^{-\frac{TR}{T_1}}\right)$ $\quad M_z(5) = 0$

So far it is clear that in order to ensure maximum contrast between tissues, it is necessary to modify TR. If there is a small difference in T_1 values:

$$d(SI) = \frac{M_o TR \cdot \left(e^{-\frac{TR}{T_1}} \right) d(T_1)}{T_1^2}$$

Now maximize with respect to TR:

$$\frac{d(SI)}{d(TR)} = 0 = M_o \left(\frac{e^{-\frac{TR}{T_1}}}{T_1^2} - \frac{TR \cdot e^{-\frac{TR}{T_1}}}{T_1^3} \right) d(T_1)$$

$$0 = \frac{e^{-\frac{TR}{T_1}}}{T_1^2} \left(1 - \frac{TR}{T_1} \right)$$

$$TR = T_1$$

Hence, when TR = T_1, the maximum contrast is acquired between two tissues which have similar T_1 values.

If TR is decreased, more averages can be applied (which decreases the noise) in the same imaging duration. However, the decrease in TR will decrease the contrast between the tissues. It is necessary to optimize these two conflicting parameters:

$$\text{Give: } SNR \propto \sqrt{N}; \quad N \propto \frac{1}{TR} \text{ then}$$

$$SNR \propto \sqrt{\frac{1}{TR}}$$

$$\Rightarrow d(SNR) = \sqrt{\frac{1}{TR}} \frac{TR \cdot e^{-\frac{TR}{T_1}}}{T_1^2} d(T_1) = \frac{\sqrt{TR} e^{-\frac{TR}{T_1}}}{T_1^2} d(T_1)$$

Now maximize with respect to TR:

$$\frac{d(SNR)}{d(TR)} = \frac{e^{-\frac{TR}{T_1}}}{2\sqrt{TR}T_1^2} - \frac{\sqrt{TR}e^{-\frac{TR}{T_1}}}{T_1^3} = 0$$

$$\Rightarrow TR = \frac{T_1}{2}$$

(Rosen, 2006)

APPENDIX C

STUDY INFORMED CONSENT

Araştırmanın adı: Beynin yaşlanması sürecine ait MR görüntülerinde WM-GM kontrastını iyileştirmek için görüntüleme parametrelerinin optimizasyonu

Sorumlu araştırmacı: Yrd. Doç. Dr. Didem Gökçay

Araştırmanın yapılacağı yer: ODTÜ Enformatik Enstitüsü, Bilkent UMRAM MR Merkezi

Orta Doğu Teknik Üniversitesi Biyomedikal Mühendisliği bölümü yüksek lisans öğrencisi Hayriye AKTAŞ tarafından, Orta doğu Teknik Üniversitesi Enformatik Enstitüsü Öğretim Üyelerinden Yrd. Doç. Dr. Didem Gökçay'ın danışmanlığında ve yine Orta doğu Teknik Üniversitesi Biyolojik Bilimler Bölümü Öğretim Üyelerinden Doç. Dr. Havva Doğru'nun ortak danışmanlığında, yüksek lisans tezi kapsamında beynin yaşlanması sürecine ait MR görüntülerinin kontrastını iyileştirmek için planlanan bu araştırma projesine katılmak için davet edilmektesiniz. Çalışma sadece sağlıklı yetişkinleri kapsamaktadır ve çalışmaya 15 gönüllü katılacaktır.

Beyin görüntülemesi UMRAM MR Merkezi'nde bulunan ve beyin görüntülemeye yarayan MR cihazı yardımıyla yapılacaktır ve herhangi bir potansiyel risk içermemektedir. MR cihazında bilindiği üzere, herhangi bir radyoaktif madde ya da X-ışını kullanılmaz, klinik olarak günlük hayatımızda pek çok uygulamaları vardır.

MR çekimi öncesinde katılımcılara toplamda yaklaşık 10 dakika sürecek olan geriatrik depresyon ölçeği ve standardize mini mental test uygulanacaktır. Daha sonra, katılımcılardan yatar pozisyonda başlarına bir aygıt giydirilerek, MR cihazında yatmaları istenmektedir.

MR çekimi, uygun önlemler alındığı takdirde zararsız bir işlemdir. Ancak kapalı yer korkusu olan kişilerin ve vücudunda metal protez, kalp pili, diş teli gibi metal cihazlar bulunan kişiler çalışmaya katılamazlar. MR çekimi başladığında ritmik sesler duyacaksınız. Personel bu sesi azaltmak için size kulak tıkacı temin edecektir. Cihazın içerisinde, iletişim yapabilmeniz için yerleştirilmiş bir ses sistemi bulunmaktadır. Bu vesileyle teknisyen ile konuşmanız mümkündür. Çekim süresince hiçbir kafa hareketi olmaması gerekmektedir. Öksürme, boğazı temizleyecek şekilde yutkunma gibi hareketler çekim kalitesini düşürdüğünden, bazı çekimlerin tekrarlanması gerekebilir. Bu nedenle mümkün olduğunca kafanızı kıpırdatmamanız gerekmektedir. Bu uygulama yaklaşık olarak 40 dakika sürecek olup, kesinlikle size herhangi bir fiziksel zarar vermeyecektir.

Bu çalışmada hakkınızda edinilen tüm bilgiler gizli tutulacak ve sadece araştırmacıların bilgisine sunulacaktır. Bu çalışmadan herhangi bir rapor veya yayın yapılması halinde okuyucuların sizleri tanımasına yol açacak hiçbir kişisel bilgi bulunmayacaktır.

Deney, genel olarak kişisel rahatsızlık verecek unsurlar içermemektedir. Ancak, katılım sırasında herhangi bir nedenden ötürü kendinizi rahatsız hissederseniz yanınızda duracak mikrofona sesli komut vererek deneyi yarıda bırakıp çıkmakta serbestsiniz. Araştırmaya katılımınız tamamıyla gönüllülük çerçevesinde olup, istediğiniz zaman, hiçbir yaptırım veya cezaya maruz kalmadan, hiçbir hak kaybetmeksizin araştırmaya katılmayı reddedebilir veya araştırmadan çekilebilirsiniz. Çalışmaya katılmamayı da seçebilirsiniz.

Deney sonunda, bu çalışmayla ilgili sorularınız cevaplanacaktır. Bu çalışmaya katıldığınız için şimdiden teşekkür ederiz. Çalışma hakkında daha fazla bilgi almak için veya herhangi bir sorunuz olduğunda, Orta Doğu Teknik Üniversitesi Biyomedikal Mühendisliği bölümü yüksek lisans öğrencisi Hayriye AKTAŞ (Tel: 0551 211 40 57, E-posta: haktas@metu.edu.tr), ODTÜ Enformatik Enstitüsü Öğretim Üyesi Yrd. Doç. Dr. Didem Gökçay (Oda: A-216, Tel: 03122103750, E-posta: didemgokcay@ii.metu.edu.tr ile iletişim kurabilirsiniz.

Bilgilendirilmiş Gönüllü Olur Formu'ndaki tüm açıklamaları okudum. Yukarıda konusu ve amacı belirtilen araştırma ile ilgili tüm yazılı ve sözlü açıklama aşağıda adı belirtilen araştırmacı tarafından yapıldı. Bu çalışmaya tamamen gönüllü olarak katılıyorum ve istediğim zaman gerekçeli veya gerekçesiz olarak yarıda kesip çıkabileceğimi veya kendi isteğime bakılmaksızın araştırmacı tarafından araştırma dışı bırakılabileceğimi biliyorum. Verdiğim bilgilerin bilimsel amaçlı yayınlarda isim bilgilerim olmadan kullanılmasını, görüntü kayıtlarıma sadece araştırmacı veya etik kurul tarafından gizli tutulmak kaydıyla erişilebilmesini kabul ediyorum. Kendi özgür irademle, hiçbir baskı ve zorlama olmadan "Beynin yaşlanması sürecine ait MR görüntülerinde WM-GM kontrastını iyileştirmek için görüntüleme parametrelerinin optimizasyonu" adlı çalışmaya katılmayı kabul ettiğimi ve bu formun bir kopyasının bana verildiğini aşağıdaki imzamla beyan ederim.

Gönüllü:

Adı Soyadı: Tarih İmza

----/----/-----

Adres ve telefon:

Tanıklık Eden Yardımcı Araştırmacı:

Adı Soyadı: Tarih İmza

----/----/----

APPENDIX D

PERSONAL INFORMATION FORM FOR PARTICIPANT

Tarih:

Değerlendirici:

SOSYO-DEMOGRAFİK BİLGİLER

Adı – Soyadı: **Cinsiyeti:**

Doğum tarihi ve yaşı: **Doğum Yeri:**

Eğitim düzeyi (yıl olarak):

İş durumu: **Medeni durum:**

☐Ücretli çalışıyor ☐Serbest çalışıyor ☐ Evli ☐ Bekar

☐Ev hanımı ☐Normal emekli ☐ Boşanmış ☐ Eşi Ölmüş

☐Malulen emekli ☐İşi yok ☐ Ayrı yaşıyor

İkamet adresi:

Telefon numarası: Cep telefonu:

Ev telefonu:

e-posta adresi:

APPENDIX E

APPROVAL OF ETHICS COUNCIL

ANKARA ÜNİVERSİTESİ TIP FAKÜLTESİ KLİNİK ARAŞTIRMALAR ETİK KURUL KARARI

BAŞVURU BİLGİLERİ	ARAŞTIRMANIN AÇIK ADI	Beynin yaşlanması sürecine ait MR görüntülerinde WM-GM kontrastını iyileştirmek için görüntüleme parametrelerinin optimizasyonu			
	ARAŞTIRMA PROTOKOL KODU				
	KOORDİNATÖR/SORUMLU ARAŞTIRMACI UNVANI/ADI/SOYADI	Yrd.Doç.Dr.Didem Gökçay			
	KOORDİNATÖR/SORUMLU ARAŞTIRMACININ UZMANLIK ALANI	Bilgisayar Enformasyon Bilimi ve Mühendisliği			
	KOORDİNATÖR/SORUMLU ARAŞTIRMACININ BULUNDUĞU MERKEZ	ODTÜ Enformatik Enstitüsü Bilişsel Bilimler Bölümü			
	DESTEKLEYİCİ				
	DESTEKLEYİCİNİN YASAL TEMSİLCİSİ				
	ARAŞTIRMANIN FAZI	FAZ 1	☐		
		FAZ 2	☐		
		FAZ 3	☐		
		FAZ 4	☐		
	ARAŞTIRMANIN TÜRÜ	Yeni Bir Endikasyon	☐		
		Yüksek Doz Araştırması	☐		
		Diğer ise belirtiniz: Laboratuar Tarama Çalışması			
	ARAŞTIRMAYA KATILAN MERKEZLER	TEK MERKEZ ☐	ÇOK MERKEZLİ ☒	ULUSAL ☒	ULUSLARARASI ☐

Hasan TUNA
A. Ü. Tıp Fakültesi
İdari Personel Görevlisi

Sayfa 1

	Belge Adı	Tarihi	Versiyon Numarası	Dili
DEĞERLENDİRİLEN BELGELER	ARAŞTIRMA PROTOKOLÜ			Türkçe ☐ İngilizce ☐ Diğer ☐
	BİLGİLENDİRİLMİŞ GÖNÜLLÜ OLUR FORMU			Türkçe ☐ İngilizce ☐ Diğer ☐
	OLGU RAPOR FORMU			Türkçe ☐ İngilizce ☐ Diğer ☐
	ARAŞTIRMA BROŞÜRÜ			Türkçe ☐ İngilizce ☐ Diğer ☐

	Belge Adı		Açıklama
DEĞERLENDİRİLEN DİĞER BELGELER	TÜRKÇE ETİKET ÖRNEĞİ	☐	
	SİGORTA	☐	
	ARAŞTIRMA BÜTÇESİ	☐	
	BİYOLOJİK MATERYEL TRANSFER FORMU	☐	
	HASTA KARTI/GÜNLÜKLERİ	☐	
	İLAN	☐	
	YILLIK BİLDİRİM	☐	
	SONUÇ RAPORU	☐	
	GÜVENLİLİK BİLDİRİMLERİ	☐	
	DİĞER:	☐	

KARAR BİLGİLERİ	**Karar No:13-416-12**	**Tarih: 27 Ağustos 2012**
	Yukarıda bilgileri verilen klinik araştırma başvuru dosyası ile ilgili belgeler araştırmanın gerekçe, amaç, yaklaşım ve yöntemleri ile bilgilendirilmiş gönüllü olur formu incelenmiş çalışmanın başvuru dosyasında belirtilen merkezlerde gerçekleştirilmesinde etik ve bilimsel sakınca bulunmadığına toplantıya katılan Etik Kurul üye tam sayısının salt çoğunluğu ile karar verilmiştir.	

ANKARA ÜNİVERSİTESİ TIP FAKÜLTESİ KLİNİK ARAŞTIRMALAR ETİK KURULU

ÇALIŞMA ESASI	Klinik Araştırmalar Hakkında Yönetmelik, İyi Klinik Uygulamaları Kılavuzu
BAŞKANIN UNVANI / ADI / SOYADI:	Prof.Dr.Mehmet MELLİ

APPENDIX F

MATLAB CODE OF T_1 ESTIMATION

```
clear all;
clc;

subjcode='s01.mat';
sinFA_firstimg=sind(3);

TR=20;
TE=4.1500;

FA1=5;
FA2=15;
FA3=30;

%%%%%%%%%%%%%%%%%%%%%%%%%%%%%%%%
% READING ALL SLICES             %
%%%%%%%%%%%%%%%%%%%%%%%%%%%%%%%%

N=20;%number of slices

im3=zeros(256,256,N);  %for memory allocation
im5=zeros(256,256,N);
im15=zeros(256,256,N);
im30=zeros(256,256,N);

cd('C:\Users\Hayriye\Documents\MATLAB\flash  trials\H3\FA3');  %
DIRECTORY CHANGING FOR IMAGES WITH FA=3
b=dir;
for j=1:N

    im3(:,:,j)=dicomread(b(j+2).name);

end

cd('C:\Users\Hayriye\Documents\MATLAB\flash    trials\H3\FA5');%
DIRECTORY CHANGING FOR IMAGES WITH FA=5
b=dir;
for j=1:N
```

```
    im5(:,:,j)=dicomread(b(j+2).name);

end

cd('C:\Users\Hayriye\Documents\MATLAB\flash   trials\H3\FA15');%
DIRECTORY CHANGING FOR IMAGES WITH FA=15

b=dir;
for j=1:N

    im15(:,:,j)=dicomread(b(j+2).name);

end

cd('C:\Users\Hayriye\Documents\MATLAB\flash   trials\H3\FA30');%
DIRECTORY CHANGING FOR IMAGES WITH FA=30

b=dir;
for j=1:N

    im30(:,:,j)=dicomread(b(j+2).name);

end


%%%%%%%%%%%%%%%%%%%%%%%%%%%%%%%%%%%%%%%%%%%%%%%%%%%%%%%%%%%%%%%%%%%%%%%
%%%%%%%%
cd('C:\Users\Hayriye\Documents\MATLAB\flash trials\H3');

im3=double(im3);
im5=double(im5);
im15=double(im15);
im30=double(im30);

img_width = 256;
img_height = 256;

final_T1 = zeros(img_width,img_height,N);


error=zeros(img_width,img_height,N);
error(:,:,:) = 99999999;

tmp_err=zeros(img_width,img_height,N);
tmp2_err=zeros(img_width,img_height,N);
tmp3_err=zeros(img_width,img_height,N);
tmp4_err=zeros(img_width,img_height,N);

t1_start = 200;
t1_end = 4000;
```

```
I5 = zeros(img_width,img_height,N);
I15 = zeros(img_width,img_height,N);
I30 = zeros(img_width,img_height,N);


for t1=200:4000;

      tmp_err(:,:,:)=0;
      tmp2_err(:,:,:)=0;
      tmp3_err(:,:,:)=0;
      tmp4_err(:,:,:)=0;

      I5(:,:,:)=(im3(:,:,:)*sind(FA1)/sinFA_firstimg)*(1-exp(-
TR/t1))/(1-cosd(FA1)*exp(-TR/t1));
     I15(:,:,:)=(im3(:,:,:)*sind(FA2)/sinFA_firstimg)*(1-exp(-
TR/t1))/(1-cosd(FA2)*exp(-TR/t1));
     I30(:,:,:)=(im3(:,:,:)*sind(FA3)/sinFA_firstimg)*(1-exp(-
TR/t1))/(1-cosd(FA3)*exp(-TR/t1));

     tmp_err(:,:,:)      =      abs((I5(:,:,:)-im5(:,:,:)))      +
abs((I15(:,:,:)-im15(:,:,:))) + abs((I30(:,:,:)-im30(:,:,:)));

     tmp2_err(:,:,:) = error(:,:,:) > tmp_err(:,:,:);
     error(:,:,:) = tmp2_err(:,:,:).*tmp_err(:,:,:);

     tmp3_err(:,:,:) = ~tmp2_err(:,:,:);
     tmp4_err(:,:,:) = tmp2_err(:,:,:)*t1;

     final_T1(:,:,:)   =   (final_T1(:,:,:).*tmp3_err(:,:,:))   +
tmp4_err(:,:,:);
     t1
end;

save(subjcode,'final_T1');
H3_final_T1=final_T1;
nii=make_nii(H3_final_T1, [1 1 1], [0 0 0]);
save_nii(nii,'H3_T1.nii');
save
%%%%%%%%%%%%%%%%%%%%%%%%%%%    to    read    anatomic    sequence
%%%%%%%%%%%%%%%%%%
cd                        ('C:\Users\Hayriye\Documents\MATLAB\flash
trials\H3\ANATOMIK2');
N=124;
b=dir;
for j=1:N

    MPRAGE(:,:,j)=dicomread(b(j+2).name);

end
cd('C:\Users\Hayriye\Documents\MATLAB\flash trials\H3');
nii=make_nii(MPRAGE, [1 1 1], [0 0 0]);
img = MPRAGE;
```

```
img = ipermute(img,[2 1 3]);
img = img(:,end:-1:1,:);
hdr = nii.hdr;
hdr.dime.dim([2 3 4]) = size(img);
nii.img = img;
view_nii(nii);
save_nii(nii,'MPRAGE.nii');
```